UNIVERSITY OF MINNESOTA
ST. ANTHONY FALLS HYDRAULIC LABORATORY
LORENZ G. STRAUB, Director

Technical Paper No. 24, Series B

THE ST. ANTHONY FALLS HYDRAULIC LABORATORY GRAVITY-FLOW FREE-JET WATER TUNNEL

by

EDWARD SILBERMAN and JOHN F. RIPKEN

August 1959
Minneapolis, Minnesota

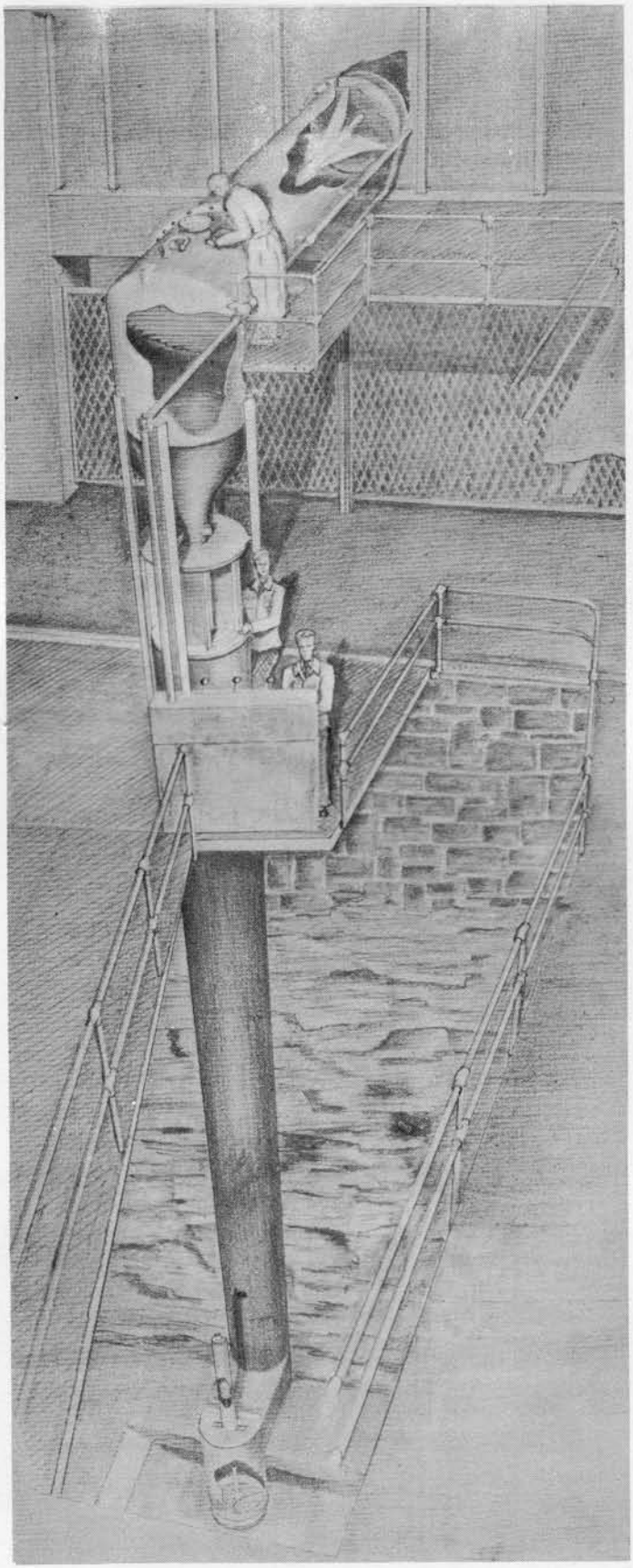

The Free-Jet Water Tunnel

UNIVERSITY OF MINNESOTA
ST. ANTHONY FALLS HYDRAULIC LABORATORY
LORENZ G. STRAUB, Director

Technical Paper No. 24, Series B

THE ST. ANTHONY FALLS HYDRAULIC LABORATORY GRAVITY-FLOW FREE-JET WATER TUNNEL

by

EDWARD SILBERMAN and JOHN F. RIPKEN

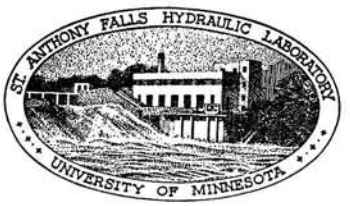

August 1959
Minneapolis, Minnesota

A B S T R A C T

A unique facility for studying cavitation phenomena has been developed at the St. Anthony Falls Hydraulic Laboratory of the University of Minnesota in the form of a gravity-flow free-jet water tunnel which makes use of the 50-ft drop in the Mississippi River at the Falls where the Laboratory is situated. The tunnel is an outgrowth of projects sponsored by the Office of Naval Research and is used for experimental studies of cavities under an exceptionally wide range of conditions, especially at small cavitation numbers. Both axially symmetric and two-dimensional test sections have been provided.

The facility differs from customary water tunnels in that the test jet is surrounded by a gas-filled chamber in which the pressure can be lowered to nearly vapor pressure of the liquid stream. Operation is entirely by gravity flow; no pumps are required either for actuating the stream or producing vacuum in the test chamber. The test jet is vertical, 40 in. long, and flows at speeds up to 50 fps. The axially symmetric jet is 10 inches in diameter, while the alternate two-dimensional jet is 5 in. thick between rigid walls and of adjustable width from 6 to 15 in. between free boundaries. A motion picture has been prepared to describe some of the tunnel features and the operating characteristics.*

---

*St. Anthony Falls Gravity-Flow Free-Jet Water Tunnel, St. Anthony Falls Hydraulic Laboratory Film No. 25, 400 ft, 16mm, Kodachrome, silent.

C O N T E N T S

LIST OF ILLUSTRATIONS

THE ST. ANTHONY FALLS HYDRAULIC LABORATORY GRAVITY-FLOW FREE-JET WATER TUNNEL

I. INTRODUCTION

A. Background

Research was undertaken at the St. Anthony Falls Hydraulic Laboratory in 1949 to explore the characteristics of various types of water-tunnel test facilities. This research resulted in special effort being directed primarily to exploring the merits of the free-jet type of water tunnel, as distinguished from the customary closed-jet and open-jet types. It may be noted that in the closed-jet tunnel the liquid traverses the test section within a solid boundary, while in the open-jet tunnel the test stream passes through a chamber of relatively static liquid surrounding the stream. Tunnels of the closed-jet and open-jet type have been used as hydrodynamic test facilities for many years. The first practical free-jet tunnel was probably constructed at Göttingen, Germany, and was described by H. Reichardt [1]* in 1945. This tunnel had a rectangular, horizontal jet with solid boundaries in the front and rear and "free" interfaces at the top and bottom. The jet was 5.9 in. wide and 7.8 in. high and had a maximum speed of about 33 fps. The jet discharged into a closed vertical steel tank where the free entrained air could settle out. The facility was actuated by a recirculating pumping unit operating on the return conduit from the tank.

The free-jet type of tunnel is especially useful for studying flow about bodies at small cavitation numbers.** This is true, first, because of an inherent resistance to cavitation of the tunnel itself. Earlier studies at the St. Anthony Falls Hydraulic Laboratory had shown that in an open-jet type of tunnel with no body in the test section, self-produced shear eddies occurred which would begin to cavitate when the cavitation number decreased much below 0.40. Similar tests in a closed-jet type of tunnel indicated that boundary wall cavitation would occur if the cavitation number decreased much below 0.05. The latter lower limit was associated with a test section of refined form and small size; it could be considerably higher for larger and

---

*Numbers in brackets refer to the List of References on p. 24.

**Cavitation number is defined by Eq. (1) on p. 5.

cruder tunnels. On the other hand, the free-jet boundary produces no cavitation whatsoever. In addition to the inherent cavitation limits of open and closed types of test section boundaries, there is a blockage problem that occurs when test bodies are placed in the test sections of these tunnels. Blockage does not occur in the free jet. The blockage problem has been fully discussed by Birkhoff, Plesset, and Simmons [2]. Even when bodies are tested without cavities, the wall corrections in the free jet are smaller in magnitude than those in a closed jet for equal-sized bodies and jets.

With a desire to study the cavitation research possibilities of a free-jet facility, the Laboratory undertook exploratory tests with a pilot experimental tunnel having a 2-in. diameter test jet. A velocity of 50 fps and pressures near vapor pressure were achieved in the pilot tunnel. The tests were elementary in nature but served to establish the following significant conclusions:

(1) Preferably the jet should be directed downward to minimize gravitational distortion of the jet and to take advantage of gravitational drainage of the test section for steady-state cavities;

(2) Nonrecirculating flow is advantageous to eliminate the possibility of recirculating air in the system and the serious flow instability that results therefrom; nonrecirculating flow also avoids water temperature rise;

(3) Effective means of recovering the kinetic energy of the jet are not apparent and this energy loss must be accepted in the design;

(4) Natural entrainment of air at the jet interface at high speeds aspirates sufficient air from the test section to permit any desired chamber vacuum without auxiliary vacuum pumping equipment;

(5) A test jet of circular cross section possesses good flow uniformity and can be effectively fitted with curved contact viewing windows;

(6) Measurements of pressure at low pressures are inherently more accurate in the free jet than in other tunnel types

because gaseous rather than liquid pressure measurements are involved, and thus cavitation does not occur in the measuring system;

(7) Useful studies of the interaction between a test body and a finite free-jet stream would require a tunnel larger than the 2-in. diameter pilot jet.

B. The Free-Jet Tunnel

On the basis of the findings of the 2-in. tunnel studies, and in view of the substantial natural water supply and head uniquely available at St. Anthony Falls on the Mississippi River, the new tunnel was designed as a nonrecirculating gravity-flow system. This was particularly advantageous because the expense of installing a variable-speed pump and drive system with power requirements of the order of 150 hp was eliminated. All of the features of the pilot model were realized in the larger tunnel. A disadvantage of this system is that during spring floods, particularly, and to a certain extent during the summer months the river water is slightly colored and carries some fine mineral and organic solids. This reduces the transparency of the stream. There is also occasional difficulty with small grass-like filaments which tend to collect on sharp edges placed in the test stream. When the river is covered by ice in the winter, the water is very transparent and there are no apparent foreign bodies in the stream.

The tunnel was originally equipped with an axially symmetric test section housing a 10-in. diameter circular jet. The tunnel with axially symmetric test section is shown in the frontispiece in an artist's rendition and schematically in Fig. 1. Figure 2 is a photograph of the axially symmetric test section. Both the basic tunnel and axially symmetric test section are described in detail in Section II, following. Within the test section test bodies are supported in the stream by an axial sting as may be seen in Figs. 9 and 10. Cavitation phenomena are observed and photographed through contact windows in the housing. No dynamometer has been provided as yet for the axially symmetric test section. Results of some investigations performed in this test section are given in a project report of the Laboratory [3].

Subsequently, the axially symmetric test section was adapted to testing two-dimensional bodies at small cavitation numbers by inserting two parallel, thin plates longitudinally and symmetrically in the 10-in. jet. The

plates were 5 in. apart, producing a nearly rectangular test stream 5 in. by 10 inches in cross section. Two-dimensional bodies spanned the 5-in. space between plates. The arrangement and some of the results obtained are described in References [4] and [5]. Although the two-dimensional results were quite useful, there were certain limitations to this tunnel arrangement, described in Reference [5], which made it desirable to work with a better two-dimensional test section.

Finally, a new, permanent, two-dimensional test-section housing was provided. The two-dimensional jet is 5 in. thick between rigid walls and of adjustable width from 6 to 15 in. between free boundaries. Figure 3 is a photograph of the two-dimensional test section which is described in detail in Section III, following. The two-dimensional test section, together with its approach pipe and nozzle, is completely interchangeable with the axially symmetric test section and nozzle. (It requires two to three days for two men to interchange the axially symmetric and two-dimensional test sections. If this change were made frequently, less time would be required.) The two-dimensional test section accepts cylindrical bodies of 5-in. span, supporting them at their ends on the rigid walls. Dynamometers of the null-balance, hydraulic load-cell type are provided for measuring lift, drag, and pitching moment. The test section is completely transparent.

The basic method of operation of the tunnel is the same regardless of the test section that is installed. As may be seen from Fig. 1, the tunnel operates by gravity, taking water from the upper river pool at St. Anthony Falls and wasting it to the lower pool. There is a total drop of 50 ft between pools. The test section is vertical and test bodies are located therein at about 34 ft above tailwater height and at eye level from the operating floor. The tunnel is operated by opening the inlet valve in the supply channel to let water into the tunnel, and the discharge valve at the downstream end of the tunnel to let it out. Water passing through the tunnel entrains the interior air and carries it out of the structure, thus reducing the test-section pressure. When the test section is sealed, the air therein is completely removed by the falling jet, and the pressure is reduced to the vapor pressure of water by the weight of the water column suspended in the vertical pipe acting as a barometer. Pressures between vapor pressure and atmospheric pressure are obtained by admitting controlled quantities of atmospheric air to the test section, thereby balancing the entraining action of the jet and

lowering the water column. The aspirating action is so effective that pressures near vapor pressure can be obtained in a few seconds after sealing the test section. A stable pressure level is readily maintained by controlling the pressure bleed valves visible in Figs. 2 and 3. The maximum velocity available in the tunnel is 50 fps, but this maximum is reduced as the operating pressure is increased by admitting air. At a given operating pressure, any velocity below the maximum may be obtained by control of the water-inlet valve. The usual operating range is between 30 and 50 fps. (At velocities below about 30 fps, secondary gravitational effects may become important.)

The test-section gas pressure is transmitted throughout the jet, maintaining the jet at uniform pressure. By measuring the test-section pressure p_o and the test stream velocity at body height V_o, a cavitation number for any test body is obtained from the formulas:

$$\sigma_v = \frac{p_o - p_v}{q} \tag{1a}$$

$$\text{or } \sigma = \frac{p_o - p_k}{q} \tag{1b}$$

where σ or σ_v is the cavitation number,

p_v is the vapor pressure of water at the operating temperature,

p_k is the measured cavity pressure (for quasi-steady cavities),

$q = \rho V_o^2/2$ is the reference dynamic pressure, and

ρ is the density of water.

Only Eq. (1a) can normally be used when a test body exhibits bubble cavitation. (Small bubbles form at random near the low pressure region and collapse downstream.) This tunnel is most useful at small cavitation numbers where long, quasi-steady, hollow cavities form behind a body. It is known that in such cavities the internal pressure tends to be somewhat higher than vapor pressure. Under these circumstances, Eq. (1b) is preferable as a definition for cavitation number. The tunnel test sections permit measuring internal cavity pressures p_k for use in Eq. (1b).

Fortunately, low pressure and high velocity occur simultaneously in this free-jet tunnel. Consequently, it is easy to obtain extremely low cavitation numbers. In the two-dimensional test section, test bodies can actually

be studied at zero cavitation number. This is accomplished by simply splitting the jet so that the cavity literally extends to infinity and the cavity pressure and chamber pressure are equal to each other. The axially symmetric jet cannot be split while retaining axial symmetry. If the cavity is not split, there is a minimum workable cavitation number that is obtainable in the tunnel. This minimum is, however, considerably lower than for an equivalent closed- or open-jet tunnel. The working minimum is determined by the requirement that the cavity should not exceed the approximately 40-in. length of the test section, and hence depends on the body under test. A 45-degree 1/4-in. cone has been tested in the axially symmetric test section at σ = 0.005. In the two-dimensional test section, an equally low cavitation number has been obtained with a hydrofoil of 2.5-in. chord at a 2-degree angle of attack.

The water jets in both the axially symmetric and two-dimensional test sections are quite turbulent. The turbulence is believed to originate in the flow through the inlet valve. Turbulence spheres of 2-in. and 1-1/4-in. diameter were used in the axially symmetric jet in order to obtain a quantitative estimate of this turbulence. The sphere boundary layer was assumed to pass through critical when the wake pressure coefficient rose to 1.22 (corresponding to a drag coefficient of 0.3). Transition occurred at 20 and 36 fps on the 2-in. and 1-1/4-in. spheres, respectively, indicating a critical Reynolds number of the order of 200,000.

C. Personnel

The gravity-flow free-jet tunnel in its present form is the result of the combined efforts of many people, and this paper is a condensation of reports prepared by several of them. Lorenz G. Straub, Director of the Laboratory, was instrumental in the general planning for the tunnel and in securing support for its construction. John F. Ripken was largely responsible for the original design concepts and has been concerned more or less actively with all subsequent modifications. Charles D. Christopherson conducted the pilot model studies and prepared the original report describing the tunnel and axially symmetric test section. Edward Silberman conceived and planned the two-dimensional test section. Ernest Elguther prepared most of the detail design drawings, and Joseph Bauer performed much of the most difficult machine work. In addition, many of the research assistants and shop people at the

Laboratory have contributed to the routine work of testing, assembling, and disassembling the various tunnel components during the developmental stages.

Construction of the tunnel was made possible through the assistance of the Office of Naval Research, United States Department of the Navy, under Contracts N6 onr-246, Task Order VI, and 710(24).

II. THE TUNNEL AND AXIALLY SYMMETRIC TEST SECTION

A. The Tunnel Structure

Some of the general features of the free-jet tunnel structure have already been described in Section I and shown in the Frontispiece and in Figs. 1, 2, and 3. The bulk of the structure is welded from structural steel plate and pipe. Referring to Fig. 1, the tunnel consists of two major sections. There is an upper section consisting of the inlet valve, horizontal conduit, miter elbow, and a short section of 30-in. diameter pipe. This is supported by the wall of the headwater pool at one end and at the other by a set of four columns, some of which are visible in Figs. 2 and 3, anchored to the Laboratory foundation. The lower section of the tunnel consists of a long vertical conduit and discharge valve. The lower section is independently anchored to the Laboratory foundation. The test sections, together with their nozzles, are fitted between the upper and lower sections of the tunnel.

The inlet valve is pushed open and held in that position by a hydraulic cylinder. The valve is closed by water pressure in the headpool when pressure is released in the cylinder. Pressure in the cylinder is built up using a hand pump. One stroke of the pump opens the valve about 1/8 inches. The valve is usually opened from 3/4 to 3 in. during tunnel operation. The hydraulic control system for operating the inlet valve, as well as other tunnel components, is shown schematically in Fig. 4. The control system is housed in a stand, shown in Fig. 5, the back of which is visible in Figs. 2 and 3. The stand contains indicating dials showing the position of the inlet and discharge valves at all times. These dials are cable-operated from the valves.

The guide vanes, which form an integral part of the miter elbow, are of the circular segment type. They are supported along the miter at their outer ends by being tack-welded to the walls of the elbow, and along the elbow axis by being welded to a faired splitter which in turn is welded to the elbow walls at both corners of the bend. Specifications for the vanes and

splitter, which are fabricated from stainless steel, are given in Fig. 6. At the top of the horizontal leg of the elbow, a short 6-in. diameter circular pipe has been fitted to the elbow wall and covered with a transparent acrylic resin plate. This arrangement permits visual inspection of the guide vanes and easy access to them for cleaning purposes. The pipe also acts as an air-collection dome, trapping bubbles produced by the high-speed flow through the annular valve opening. Collected air is sucked off by vacuum from an external source. A thermometer well for obtaining water temperature is also provided at the miter elbow.

The vertical conduit of the lower-tunnel section is divided into two parts at the operating-floor level by a short rubber pipe coupling. Each part is independently supported from the foundation. The rubber coupling prevents vibrations generated by the air-entraining action from reaching the test section.

The tunnel discharge valve is also hydraulically actuated. Pressurizing the hydraulic cylinder closes the valve and the valve opens by gravity and water weight when pressure is released. This valve is normally used fully open--about 5 inches. Its main use is to close the tunnel when water is diverted for calibration. However, it may also be used in connection with the inlet valve and air-bleed valves to control tunnel velocity and pressure. The test section of the tunnel can actually be flooded by use of the discharge valve, causing the tunnel to operate as a low-speed open-jet facility.

B. The Axially Symmetric Test Section and Nozzle

The axially symmetric test section and nozzle are installed together in the tunnel, and have been shown in Fig. 2. The nozzle contracts the flow from the 30-in. supply pipe to the 10-in. test-stream diameter. The nozzle terminates 40 in. above the entrance to the discharge pipe in a 30 in. O. D. flange.

The contraction form is the result of Laboratory studies conducted several years ago on open- and closed-jet tunnels. The form is shown in Fig. 7 together with its boundary-pressure distribution characteristics taken from the earlier studies. These studies showed the pressure to be a monotonically decreasing function of the distance from its upstream end with no significant zones of flow separation. More important, the studies established that there

is good uniformity of pressure and velocity distribution in the discharge flow.

The contraction is an aluminum casting smoothly machined to the design profile. Three sets of piezometer taps were carefully machined into the contraction at 1-1/2, 30-1/2, and 45-3/4 in. from the upstream end as shown in Fig. 7. Each set consisted of four taps located at 90 degrees on a circumference. The taps are used for velocity calibration as described later.

The 10-in. diameter jet issuing from the nozzle is shown in Fig. 8. The test-section elements are primarily intended to provide suitable support to test bodies and instruments in the jet, and to provide an evacuated housing which allows convenient viewing of and access to the test bodies. Bodies are sting-supported along the axis of the jet as illustrated in Fig. 9. They may be placed at any height in the jet.

As may be seen in Fig. 8, observation of bodies in the stream is limited by turbulence on the jet surface, and contact viewing windows are necessary to see into the jet. A contact window may be seen in place at the right side of Fig. 9. Windows are machined from Plexiglas sheets 1-1/2 in. thick and 12 in. wide, selected to have one optically smooth surface. Each sheet is finished to 5-in. radius on its poorer surface over about 52 degrees of arc. The sheets are sealed to an aluminum frame and installed so that the curved surface just contacts the jet over its 40-in. test length.

Windows may be placed at any of four positions around the jet, each 90 degrees from the adjacent positions; normally, only one window is used at a time. The upper end of each window is very carefully aligned with the end of the nozzle, and practically no cavitation occurs at this juncture. Velocity traverses in the jet, described later, have established that the limited contact area of the window does not significantly distort the core flow in the upper regions of the test jet. Nor does the contraction of the jet from gravitational acceleration break the contact with the vertical window. Figure 10 illustrates the viewing potential of the window system. Scale distortion is negligible as has been shown by photographing a ruled grid placed in the flow.

The body supports, viewing windows, and associated instrumentation are largely suspended from the flange at the end of the nozzle. These elements and the test jet are enclosed in a plated-steel cylindrical hull which is free to telescope vertically over the discharge pipe. The hull is 24-1/2

inches in inside diameter. When closed, the hull is sealed to the nozzle flange at the top and to the discharge pipe at the bottom, permitting evacuation of the test chamber. When the hull is lowered, full access is obtained to the test section. (The hull is shown partially opened in Fig. 9.) The hull is closed by hydraulic cylinders operated from the control stand shown in Fig. 5 as indicated schematically in Fig. 4, and is opened by gravity when pressure is released from the cylinders. The hull must be closed during tunnel operation. The operation of opening the hull for full access to the test body and closing it again usually requires less than five minutes of time.

The hull is breached with four large, vertical, rectangular holes. These are aligned with the contact window positions in the jet and may be sealed to the frames of the windows. Alternatively, if contact windows are not in place, the holes must be covered with Plexiglas or metal covers. The former are used for lighting and the latter are used for auxiliary breachings for instruments and air supply vents as may be seen in Fig. 2.

Chamber pressure is measured in the axially symmetric test section by a tube suspended in the chamber from the nozzle flange. Cavity pressure is measured by tappings in the sting support system and body.

C. Calibration and Quality Tests in the Axially Symmetric Test Section

Flow through the tunnel contraction yields boundary-pressure differentials which are functionally related to the velocity of the stream discharging into the tunnel test section. Initial tests were required to establish this functional relation and to determine the flow quality of the test jet.

To implement these tests the contraction was fitted with boundary-pressure taps as shown in Fig. 7. The three sets of taps could be connected in various combinations to an external manometer which permitted a sensitive reading of the differential pressure for a wide range of discharge velocities. The functional relation between manometer readings and velocity was evaluated by diverting the exit flow from the lower leg of the tunnel into the Laboratory's gravimetric flow measuring system where the flow was precisely measured.

The results of the calibration are shown in Fig. 11 in which the mean test system velocity is defined as the flow rate divided by the exit discharge area. The capacity of the gravimetric system did not permit calibration of the contraction to the full range of tunnel velocity ($V_{o\ max}$ = 50 fps),

but the extrapolation in Fig. 11 appears fully justified. Since test bodies are located below the end of the contraction and flow in the free jet is accelerated by gravity, the actual velocity head at a test body is greater than that obtainable from Fig. 11 by the distance from the contraction to the body.

To implement the jet quality studies a special Pitot-static tube was fabricated to permit insertion into the jet via any one of the three test-section access plates shown in Fig. 2. In Fig. 2 the instrument is shown mounted in the upper access hole in which the nose of the Pitot-static tube is 2.75 in. downstream of the contraction exit. Figure 12 shows the mechanism which permitted the instrument tube to be either traversed radially or swept in an arc across the jet.

The tests reported here were made with the contact windows and traverse lines positioned as shown in Fig. 13. Figure 13 also shows the velocity traverse data. In this the velocity is expressed as the ratio of the mean velocity V_o as indicated by the pressure drop through the contraction, to the apparent velocity indicated by the Pitot-static tube. Since the test data were run with V_o = 24.9 fps and the instrument stagnation tap was located 2.75 in. below the plane in which V_o occurred, an additive gravitational correction must be made to V_o to give the true instrument velocity condition V_{o_c}. If this correction were made the plotted data would yield a ratio of $V_{o_c}/(2gH)^{1/2} = 1.00$.

The velocity is seen to be nearly constant over the entire measurable cross section. The velocity calibration of Fig. 13 is assumed valid for all velocities above the measured velocity of 24.9 fps. Higher calibration velocities were not employed because of anticipated instrument cavitation.

Pressures surrounding the jet and within the bare jet are uniform everywhere, with or without air being admitted to the chamber. The air-inlet vent to the chamber is baffled to prevent direct discharge of the air against the jet. Minimum pressure obtainable in the chamber is a few tenths of a pound per square inch above vapor pressure.

III. THE TWO-DIMENSIONAL TEST SECTION

A. Description of the Test Section

Figure 2 is a photograph of the original axially symmetric test section and nozzle. Figure 3 is a similar photograph of the two-dimensional test

section and approach pipe. Except for the replacement of the long nozzle by a uniform approach pipe and short nozzle, and replacement of the circular test-chamber enclosure by a rectangular enclosure, no changes are required in the basic free-jet tunnel in going from the axially symmetric to the two-dimensional test section.

As already observed, the two-dimensional test section is designed to produce a rectangular jet, 5 in. thick between rigid walls and of adjustable width between free boundaries. The principal interior dimensions and some other features of the test section and its appurtenances are illustrated in Fig. 14. The test section itself is simply a rectangular parallelepiped or box fabricated from 2-in. thick Plexiglas. Since the principal load is directed inwardly, the edges are joined by rabbeting and cementing. The wide faces of the test section are additionally supported by external tie bolts anchored to vertical steel beams which are visible in Figs. 3 and 15.

The test section is connected to the 30-in. diameter approach pipe through a short, one-piece, cast-aluminum nozzle. The joint between the test section and nozzle is also rabbeted and is sealed with O-rings. Two of the inner walls of the nozzle are shaped to join smoothly with the two Plexiglas walls which form the rigid boundaries of the jet. The other two walls are flat and 24 in. apart inside. The profile of the shaped walls was obtained using two-dimensional free-streamline theory; Table I gives the co-ordinates and Fig. 14 shows the principal dimensions of the nozzle. Boundary-layer growth was ignored in obtaining these co-ordinates. The shaped walls were hand-finished, using a templet as a guide, and the juncture between nozzle and Plexiglas was further hand-smoothed after joining. Operation of the tunnel shows very little evidence of cavitation at the joint, even at vapor pressure, and no cavitation on the walls elsewhere.

The width of the jet is controlled by two sliding plates located between the nozzle and approach pipe. The plates are illustrated in Fig. 14, and one of the plate housings, together with the associated operating handwheel, may be seen extending from the tunnel in Fig. 3. Each plate moves 1/8 in. per turn of its handwheel. The plates ride on the top portion of the nozzle. The plate edges have been machined to the same shape as the nozzle in the overlap region so as to make a mechanical seal under pressure, thereby reducing leakage. (The plates are moved only when the tunnel is not in operation

TABLE I

CO-ORDINATES OF JET NOZZLE

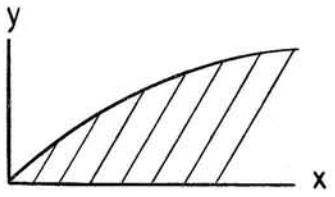

x, in.	y, in.	x, in.	y, in.
0.000	0.000	1.221	0.987
0.040	0.130	1.63	1.119
0.071	0.190	2.25	1.253
0.113	0.260	3.32	1.392
0.176	0.343	3.68	1.420
0.256	0.427	4.14	1.448
0.358	0.524	4.76	1.467
0.498	0.631	5.90	1.503
0.676	0.742	8.00	1.53 (end of nozzle)
0.914	0.863	∞	1.532

so that there is no water pressure above them during movement.) A theoretical computation has been made, using two-dimensional, free-streamline theory, giving the relation between plate opening, jet width at the test body location, and jet width at infinity. No account has been taken in the computation of the effect of gravity, but it is believed that this effect is at least partially balanced by boundary-layer development on the fixed faces of the jet. Some results of the computation are shown in Fig. 14. It is practicable to operate the tunnel in a range of jet widths from 6 in. to 15 inches. Although the jet may be placed asymmetrically in the tunnel, it is planned that operation will usually be with a symmetrically placed jet.

In order to control the test-section pressure, air is admitted to the free space on each side of the jet through holes in the nozzle casting. Admittance is through a pair of symmetrically placed 2-1/2-in. pipes fitted with valves and noise suppressors, one of which is visible in Fig. 3. Vapor pressure is obtained by closing the air valves and higher pressures are obtained by opening them to various degrees. Pressures at both sides of the jet

are equalized through a ring interconnection located immediately below the transparent test section.

The test station is centered 5-1/2 in. below the end of the nozzle, on the lateral centerline of the test section. It consists of a 3-11/16-in. diameter hole in each wide face of the test section. The holes will accept blank covers, simple trunnions, or a combination of trunnions and dynamometer elements. Figure 16 shows the tunnel in operation with blank covers at the test station; Figure 17 shows a lifting foil in place, supported by simple trunnions; while a circular cylinder supported by trunnions with dynamometer elements is shown in Fig. 15.

Covers and trunnions are Plexiglas disks, 2 in. thick, designed to form a smooth continuation of the inside tunnel walls. Each trunnion disk is especially built to hold a body of specific shape. A new pair of disks is required for each test body. Cover plates and simple trunnion disks are made to fit snugly in the holes in the test section and are aligned with the inside tunnel surface by the use of flanges cemented to the outsides of the disks. Sealing is by O-rings and a coating of grease. The trunnions may be rotated to change angle of attack; angle of attack is fixed by clamping the flanges. When dynamometer elements are used, they are used with trunnion disks whose diameters are smaller than the hole diameters. The dynamometer supports and seal rings are fitted between the outside of each trunnion and the inside of its receiving hole. The dynamometer is described in more detail beginning on p. 19.

Since test bodies extend through their supporting trunnions, it is a simple matter to provide bodies with as many integral pressure-measuring tubes as desired.

Two sets of pressure taps are provided in the test section; these are indicated in Fig. 14. One set consists of a pair of taps at test-station height, each tap being in the center of one of the narrow faces of the test section. When compared with each other, these taps can be used to assure equal pressures in the free spaces on both sides of the jet. When manifolded together, they form the basic reference pressure for work in the jet. Absolute tunnel pressure is obtained by comparing the pressure at these taps with atmospheric pressure through a U-tube manometer and by determining atmospheric pressure from an adjacent barometer. Tunnel velocity is determined by calibration, using the difference in pressure between these taps and a ring of

taps near the top of the approach pipe, visible in Fig. 3. Comparison is made through another U-tube. The calibration process is described below. Cavity pressure, for use in determining cavitation number, is also measured with reference to these taps through a U-tube.

The second set of taps consists of a row of five permanent taps along the centerline of one of the wide faces. These can be supplemented with a sixth tap insertable at the test station and a seventh in the pressure equalizing ring. The taps are used for measuring pressure gradients in the bare tunnel or within a cavity, for measuring cavity pressure when a test body does not have integral pressure tubes, and for admitting air to cavities to change cavitation number by changing cavity pressure.

The inside surface of one of the wide faces of the test section is inscribed with tick marks on a 2-in. square grid. The marks are visible in Fig. 16, for example. These marks are used to facilitate making cavity measurements in photographs.

There are six access holes in the test section, three on each narrow face. The holes are used for servicing test bodies and for inserting instruments. In Fig. 3 two of these holes on one side can be seen covered while the third is occupied by a Pitot tube. Hole covers are made flush with the inside faces of the tunnel, although only leakage flow runs down these narrow faces. Hole covers are sealed with O-rings and grease.

B. Quality of the Jet

Some effort has been given to studying the quality of the two-dimensional jet without test bodies. The first investigation was concerned with the actual width of the jet as compared to the predicted width shown in Fig. 14. As may be seen in several of the photographs, the jet is surrounded by a frothy region. This gradually merges into a narrow region of cloudy water flow, sometimes with air bubbles, near the jet. The cloudy flow penetrates slightly farther into the jet near the corners than elsewhere so that the clear, free-jet surface appears to be slightly curved across the 5-in. thickness of the jet, and the jet is not exactly rectangular in shape. The cloudy part of the jet also fans outward from the jet into the foam in a thin sheet along the rigid walls. Jet width has been measured as the average width of clear water for several operating conditions and is given in Table II.

TABLE II

MEASUREMENTS OF JET WIDTH

Plate Opening Inches	Jet Width at Bottom of Test Section, Inches			Jet Width at Test Station, Inches		
	Predicted	Measured		Predicted	Measured	
		Low Vel.	High Vel.		Low Vel.	High Vel.
9.63	6.00	4+	5-	6.01	6+	6
12.63	8.00	8	8-	8.03	9	8+
15.47	10.00	10+	10	10.06	12	11+
18.09	12.00	12	12	12.15	13.5	13.5
21.62	15.00	16+	16+	15.285	18+	18+

The discrepancies between measurement and prediction are believed to be caused by two phenomena. First, there is some leakage between the sliding plates and nozzle, especially for wide plate openings. This leakage tends to widen the jet and produces the foam surrounding the jet. (As may be seen in Fig. 8, no foam is produced in the axially symmetric test section where there is no water leakage.) Second, the region of cloudy water flow is really part of the jet and eats farther and farther into the jet because of turbulence as the flow goes downstream, reducing the apparent width of the jet. Apparently the second effect overcomes the first only for the narrowest jet. Hereafter, the jet width will be designated by the predicted width at infinity as given in Fig. 14.

There is no difficulty in balancing the pressures on the two sides of the jet. The pressure-equalizing ring at the bottom of the test section does the major part of the balancing automatically at most flows regardless of how the air valves are manipulated. When the air valves are nearly closed and the tailwater rises into the equalizing area, careful balancing must be done with the valves to prevent the jet from clinging to one side or the other of the test section. The minimum pressure surrounding the jet can be brought to within 0.2 psi of vapor pressure for the widest jets and even closer to vapor pressure for the narrower jets.

There is a small pressure gradient along the centerline of the jet when the tunnel is operated without a test body. The gradient, as measured at the wall taps, is illustrated for the 12-in. jet in Fig. 18. Figure 18 also shows the theoretical pressure distribution for a two-dimensional jet of 12-in. width at infinity. The measured and theoretical distributions are in fair agreement for the first 9 in. below the test station, but the measured pressure appears to be slightly too large thereafter until the pressure-equalizing ring is reached. It is believed that the pressure rise below 9 in. is attributable to the filling of the two-dimensional section with foam below that point. The remaining discrepancies are probably attributable to three-dimensional effects, including boundary-layer development on the rigid walls. Jets narrower than 12 in. show smaller pressure gradients, while wider jets show larger gradients than illustrated by Fig. 18.

Velocity in the jet has been calibrated and velocity distributions have been measured by use of a Pitot cylinder and a Pitot-static tube. The Pitot cylinder is a 1/4-in. diameter circular cylindrical tube with a single pressure tap at the stagnation point. It can be inserted at the test station so that the stagnation hole can be traversed across the 5-in. jet thickness between rigid walls. The Pitot-static tube was described in Fig. 12; it may be seen in place in the tunnel in Fig. 3. The tube can be inserted through any one of the three access holes on either narrow face of the test section, but only the two upper positions were used in this investigation. The uppermost position placed the stagnation hole of the tube 4 in. above the test station while the next lower position placed the stagnation hole 6-1/2 in. below the test station. The Pitot-static tube could be traversed in and out across the width of the jet and swung sideways to cover the thickness of the jet from wall to wall.

In calibrating the jet velocity, the total head reading on the jet centerline was obtained at the test station using the Pitot cylinder for a range of jet widths and water discharges. Total head readings were also obtained at the two positions above and below the test station using the stagnation hole in the Pitot-static tube. The readings above and below always differed by 10.5 in. of water, the distance between the positions, and when interpolated to the test-station position agreed with the Pitot cylinder readings. Total head was compared with static head measured at the reference taps to obtain velocity head, $V_o^2/2g$. The reference manometer reading Δh was

obtained from the mercury U-tube connecting the pressure tap ring near the top of the tunnel with the reference taps as described earlier. The calibration formula for this test section is

$$V_o^2/2g = 1.05\Delta h + 0.4 \qquad (2)$$

where $V_o^2/2g$ is measured in feet of water and Δh is measured in inches of mercury. This formula is valid for all jet widths and for tunnel velocities between 25 and 50 fps within one per cent. The corresponding formula for velocity, V_o, in fps is

$$V_o = 8.22\sqrt{\Delta h}\left(1 + \frac{0.19}{h}\right) \qquad (3)$$

The velocity head and velocity given by these formulas pertain to the edge of the free jet at the test station. At the center, the velocity may be lower by as much as 2 per cent, depending on jet width.

Total head distribution across the 5-in. jet thickness at the test station as measured by the Pitot cylinder is uniform within a small fraction of one per cent at all velocities and jet widths except in the boundary layer at each wall. The boundary layer is of the order of 1/4 in. thick. Traverses with the Pitot-static tube across the jet thickness and width were made at 40 fps velocity for 6, 10, and 12 in. wide jets; these show velocity variations up to one per cent. The variations appear to be random and it is believed that they may actually be attributable to errors in the tube which vibrates and cavitates when used at such high velocity. The Pitot-static tube could not be traversed closer than 1/2 in. to either the solid walls or free boundaries.

C. The Dynamometer

The following minimum specifications were established for the dynamometer to be used with the two-dimensional test section:

(1) Measurable load:
   a. lift--100 lbs maximum with sensitivity of 0.5 lb,
   b. drag--20 lbs maximum with sensitivity of 0.1 lb, and
   c. moment--100 in. lbs maximum about axis of test station with 0.5 in.-lb sensitivity.

(2) Model supports must not fail under twice the loading in (1) above.

(3) Surfaces of test bodies are to be visible while the dynamometer is in operation. The largest chord to be tested will be 2-1/2 inches.

(4) No leakage of outside air into the tunnel is permitted. Circulation of tunnel water or vapor within the dynamometer must be held to a minimum.

(5) Angle of attack of hydrofoils is to be set from outside the tunnel using a simple scale. Angles of ± 20 degrees must be obtainable with a sensitivity of 0.1 degrees.

(6) Because some of the hydrofoil models will be very thin, the dynamometer system must support models at both ends.

(7) The inside surfaces of the dynamometer are to be flush with the inside tunnel walls under all operating conditions.

The general appearance of the dynamometer designed to meet these specifications may be seen in Fig. 15. It is a null-balance instrument in which the test body under load is returned to its position under no load by application of external forces and moments. The external forces are applied and measured using hydraulic load cells which are calibrated in place.

The piston of the load cell, the face of which is visible in Fig. 15, is in contact with the bottom of the test-body trunnion and is in position to measure drag. Drag is measured by turning the screw visible at the bottom of the cell, thereby pushing the cell and its piston against the trunnion, until the trunnion is lifted from its supports; the pressure-gage reading then indicates the drag. The same cell is used for measuring lift by placing the cell in the empty cup at the right side of the dynamometer-support structure seen in Fig. 15. The piston of the cell then presses against the bell crank, above the empty cup, and moves the trunnion off its supports to the left. The same lift and drag apparatus may be used on the rear face of the test section. Moment is measured in the same manner as drag and lift by a cell, whose side is just visible at the right of Fig. 15, acting against a long moment arm extending from the trunnion of the dynamometer. The moment

arm is also used to set angle of attack. Cells of various load ranges can be used to measure lift, drag, or moment.

Total moment is measured by one reading on the moment cell, but lift and drag are the sums of the readings obtained at the two ends of the test body. Since all test bodies are uniformly loaded across the span in this two-dimensional tunnel, it is only necessary to read lift and drag at one end and to double the measurement. (Doubling is actually obtained in calibration as is the small moment correction to drag.) Lift and drag measurements may be made at either end using the same calibration curve.

As already noted, a test body is supported in the dynamometer by Plexiglas trunnion disks at each end of the body. Supports and seal rings are located in an annular space between the trunnion disks and receiving holes in the test section. Figure 19 shows schematically some of the details of the dynamometer arrangement. The support structure, consisting of a collar and cage assembly, is fitted to the tunnel walls, while the seal-ring assembly is attached to the trunnions. After a test body and trunnion assembly is installed in the tunnel, the seal ring is locked to the support structure by locking pins actuated by the locking ring.

Trunnion disks are permanently pinned to each test body so that their inside faces are maintained at 4.975 in. apart. The dimension 4.975 in. is used instead of 5.000 in. because measurements on the tunnel with blank covers in the dynamometer holes showed that under the normal range of operating conditions the two tunnel faces deflected inwardly a total of from 0.020 to 0.030 in. at the test station. The given dimension allows for a 0.025 in. average total deflection. The trunnion and test-body assembly can be shifted spanwise in the tunnel and held in position by thrust bearings as shown in Fig. 19. By adjusting the position of the thrust bearings during tunnel operation, the inside face of the trunnion on which lift and drag measurements are being taken can be made flush with the inside face of the tunnel. The other trunnion is then within ±0.005 in. of being flush, and any influence this projection or recess may have on lift or drag is very small because it is so far removed from the point of measurement. The spherical thrust bearings are free to roll and produce no lift, drag, or moment on the trunnions.

The cage assembly shown in Fig. 19 contains three rollers, two at the extremities of the horizontal diameter and the third at the bottom of a

vertical diameter. There is also an adjustable stop at the top of the vertical diameter. The rollers are tangent to a circle whose diameter is 0.004 in. greater than the outside diameter of the trunnion assembly at the roller position. Under load, the trunnion tends to rest on the bottom roller and on one of the two side rollers. (The seal-holding ring is more than 0.004 in. greater in ID than the trunnion so that it takes no lift or drag load.) Contact between each roller and its trunnion, as well as between the top stop and trunnion, is indicated by a light. When drag is being measured, the trunnion is raised by applying force through the load cell until the bottom roller light goes off, but not so far that the light on the top stop goes on. Lift is treated similarly. Under moment, the trunnions rotate very slightly on the rollers, twisting the formed rubber seal. Moment measurement consists of restoring the trunnions to their original position and untwisting the seal by applying force to the moment arm. To set angle of attack, the tunnel must first be shut down. The locking ring and pins, clamping the seal-holding ring to the cage, are then released and the trunnion and seal assembly may be rotated freely to any desired position, using the moment arm as a lever. The setting is completed by reclamping the seal-holding ring. For purposes of setting and measuring angle of attack, the moment arm together with its load cell is rotated up and down by a screw and rack attached to a corner of the test section.

The formed rubber seal performs its sealing task by expanding under the action of the pressure difference between the outside and inside of the tunnel and thereby blocking the annular cavity. The greater the pressure difference, the tighter the seal. When a trunnion is returned to its null position for load measurement, the seal itself carries no load. (Even when deformed, the rubber seal carries an insignificant load.) No leakage has been detected from the outside through the seal. Since atmospheric pressure exists symmetrically everywhere outside the seal, there is no net force on the trunnions from this source.

There may be an unbalanced pressure in the remaining annular space between the seal and the inside of the tunnel, however. The annular clearance in the two narrow gaps near the inside face averages about 0.003 inch. (An indicating light is used to show whether the gap is closed at any point. This light is necessary only during initial installation and adjustment of a test-body and trunnion assembly to assure that all of the load is supported on the

rollers.) Because of its large diameter the annular opening is exposed to a nearly uniform pressure around its periphery, except where a cavity crosses the opening. The uniform pressure is tunnel ambient pressure while the cavity pressure is less than ambient, the difference between the two decreasing as the cavitation number decreases as shown by Eq. (1), p. 5. At zero cavitation number, when loads are smallest, there should be no unbalanced pressure. The maximum imbalance occurs when a cavity is so short that it just crosses the annular gap before closing. The effect of pressure imbalance should be felt in the drag measurement. A rough estimate of this effect may be made as follows:

Let it be assumed that, because of the two small annular gaps on each trunnion, the full effect of pressure imbalance is felt only over that part of the gap equal to maximum cavity thickness and of depth equal to the depth to the second gap, while there is no imbalance elsewhere. (Actually, the pressure imbalance will never reach the full difference between ambient and cavity pressure because of pressure drop through the gaps, but the pressure difference will also be spread over a larger part of the gap than assumed herein.) Then, on each trunnion,

$$\text{Drag} \approx (p_o - p_k)\, t\, \frac{0.25}{12} \qquad (4)$$

where t is cavity thickness and the depth to the second gap is 0.25 inch. Since the drag is measured at one end of the body only, only the drag at that end needs to be subtracted from the total drag as may be seen from the drag-distribution sketch in Fig. 19. If Eq. (4) is put in the form of a correction to body drag coefficient, C'_D, by dividing by the dynamic pressure times body area, there results:

$$C'_D = \frac{p_o - p_k}{\rho V_o^2/2} \cdot \frac{t}{c} \cdot \frac{0.25}{5} = 0.05\, \frac{t}{c}\, \sigma \qquad (5)$$

where c is the characteristic body length and the body span is 5 inches. For a 1/2-in. diameter circular cylinder, where $t/c \approx 1$, the cavity crosses the gap at $\sigma \approx 0.5$. Here $C_D \approx 0.75$ and $C'_D/C_D \approx 3$ per cent. For a flat-plate hydrofoil of 2.5-in. chord at 8-degree angle of attack, the cavity first crosses the gap at $\sigma \approx 0.3$, $C_D \approx 0.06$, and $t/c \approx 0.2$, giving $C'_D/C_D \approx 5$ per cent. These are estimates of maximum error.

A few tests of the drag of the 0.54-in. diameter circular cylinder shown in Fig. 15 have been made. The measurements were compared with earlier measurements in a tunnel with a different test-section configuration using a strain-gage type of dynamometer [5]. Both the earlier data and present data scatter and overlap sufficiently that a 3 per cent difference would not be recognized. No other test comparisons are available at this time.

There is also a tare drag on the inside faces of the trunnions. This is readily computable with small error from turbulent boundary-layer theory; the method of computation has been given in Reference [5].

LIST OF REFERENCES

[1] Reichardt, H. On Cavitation Tunnels for Small Cavitation Numbers. Kaiser Wilhelm Institute for Fluid Motion Research, Göttingen, Germany. February 1945. Translated by N. Simmons. Issued by Royal Aircraft Establishment, London. November 1945.

[2] Birkhoff, G., Plesset, M., and Simmons, N. "Wall Effects in Cavity Flow--I." Quarterly Applied Mathematics, 8, Section 2, pp. 151-168. 1950.

[3] Self, M. W., and Ripken, J. F. Steady-State Cavity Studies in a Free-Jet Water Tunnel. University of Minnesota, St. Anthony Falls Hydraulic Laboratory Project Report No. 47. July 1955. 46 pages. (Not available except through interlibrary loan.)

[4] Ripken, J. F. Experimental Studies of a Hydrofoil Designed for Supercavitation. University of Minnesota, St. Anthony Falls Hydraulic Laboratory Project Report No. 52. September 1956. (Not available except through interlibrary loan.)

[5] Silberman, E. "Experimental Studies of Supercavitating Flow about Simple Two-Dimensional Bodies in a Jet." Journal of Fluid Mechanics, 5, pp. 337-54. 1959.

F I G U R E S

(1 through 19)

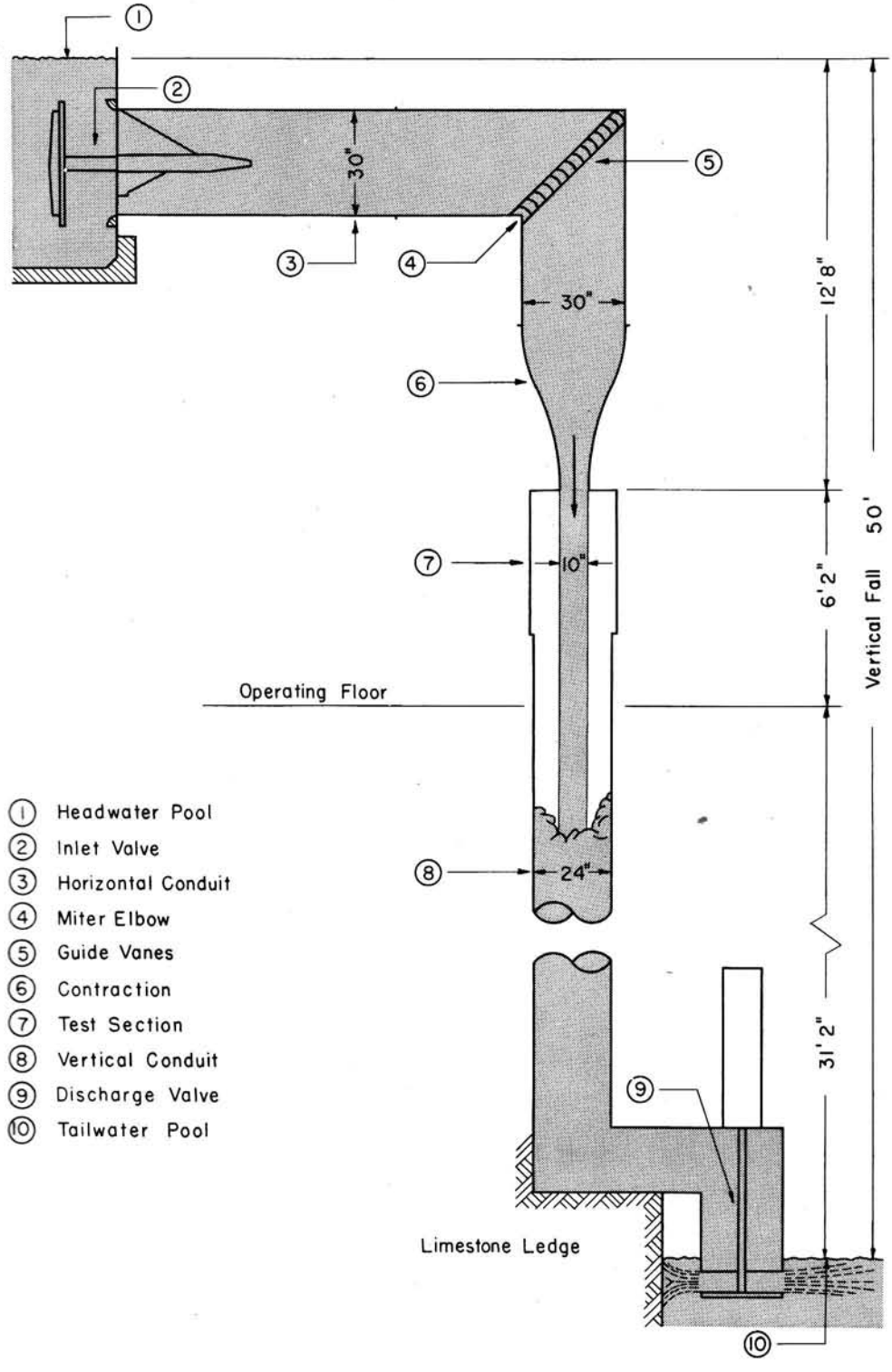

Fig. 1 - Schematic Diagram of Free-Jet Water Tunnel

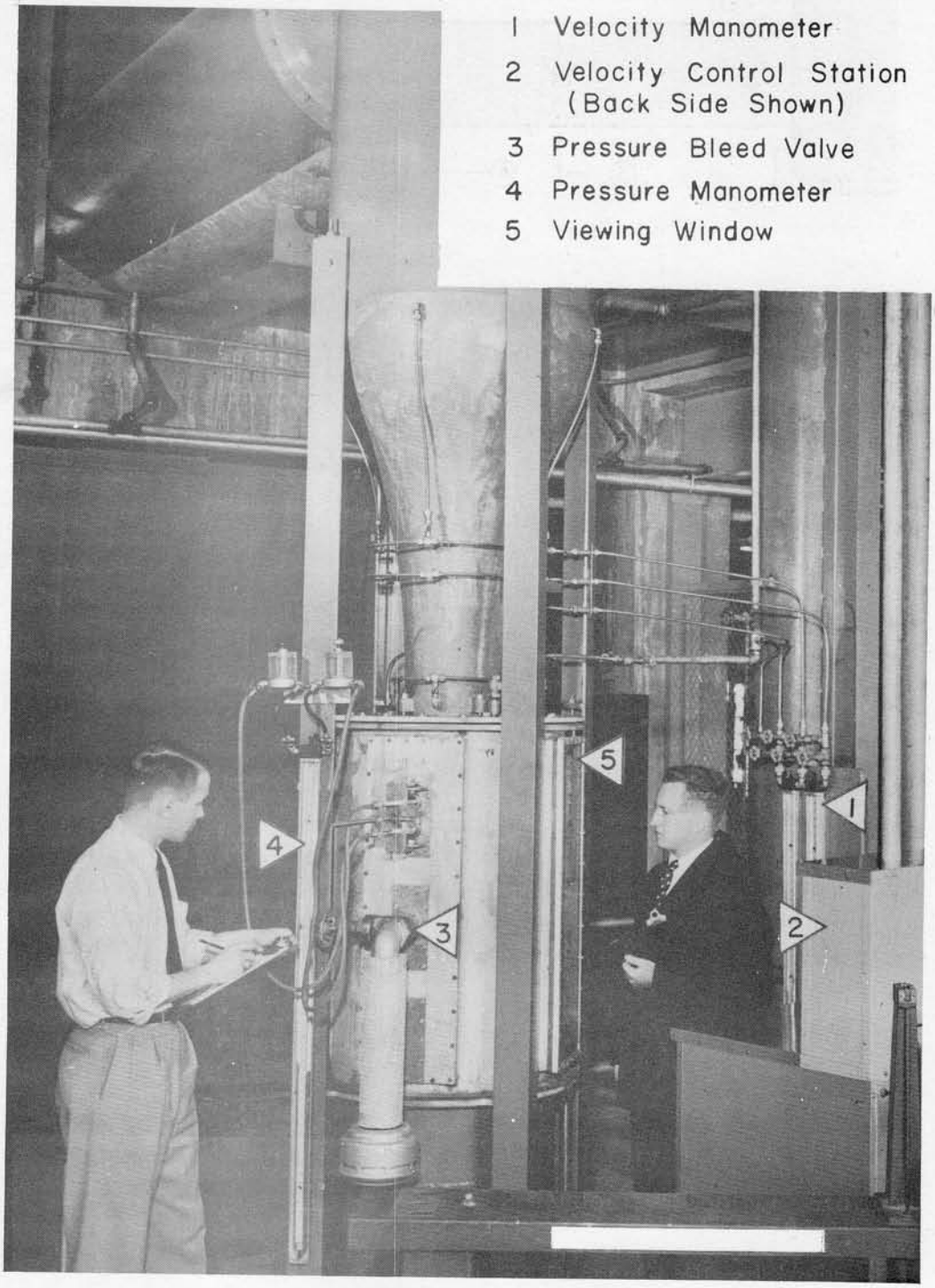

Fig. 2 - The Axially Symmetric Test Section

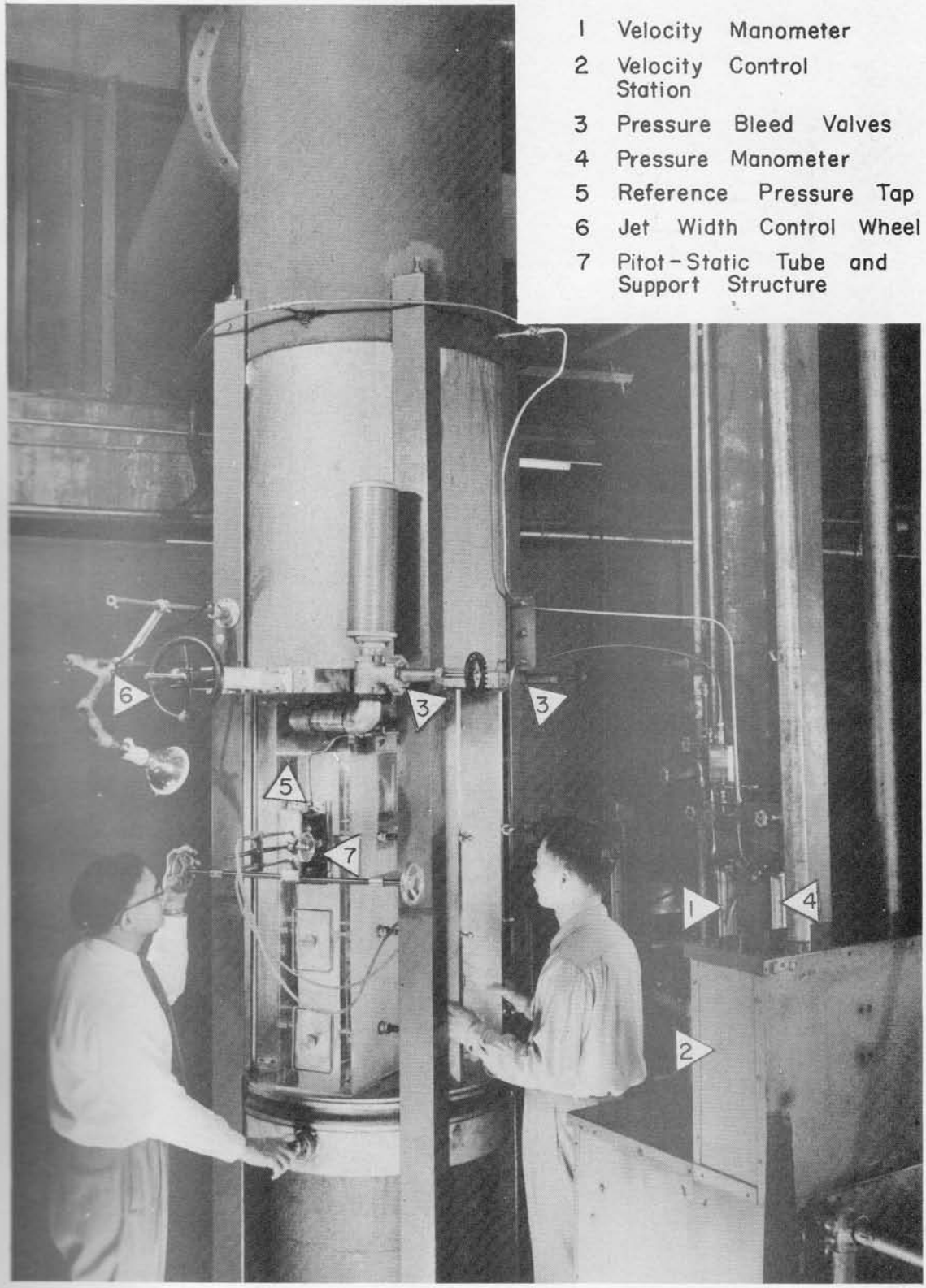

Fig. 3 - The Two-Dimensional Test Section

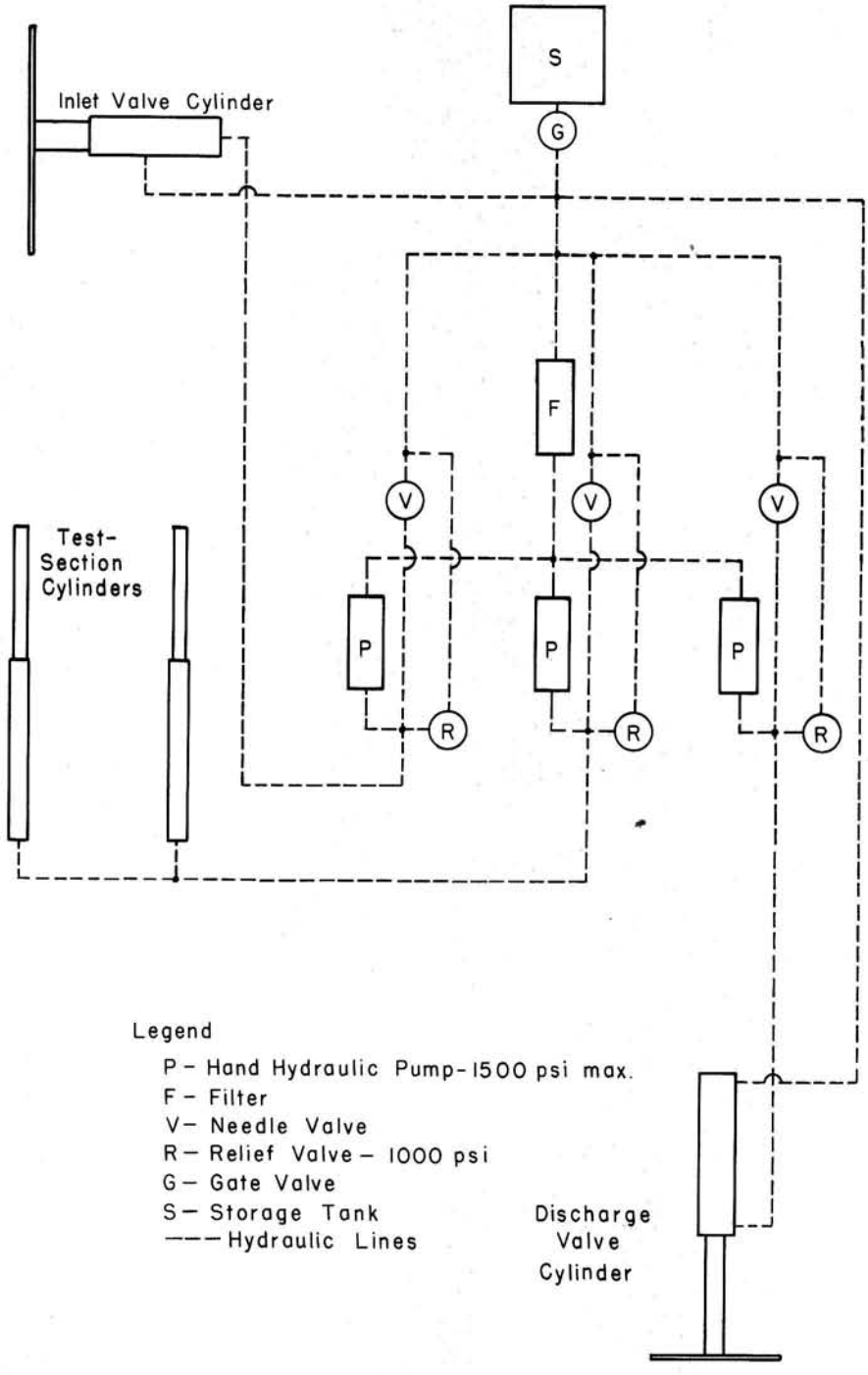

Fig. 4 - Schematic Layout of Hydraulic Control System

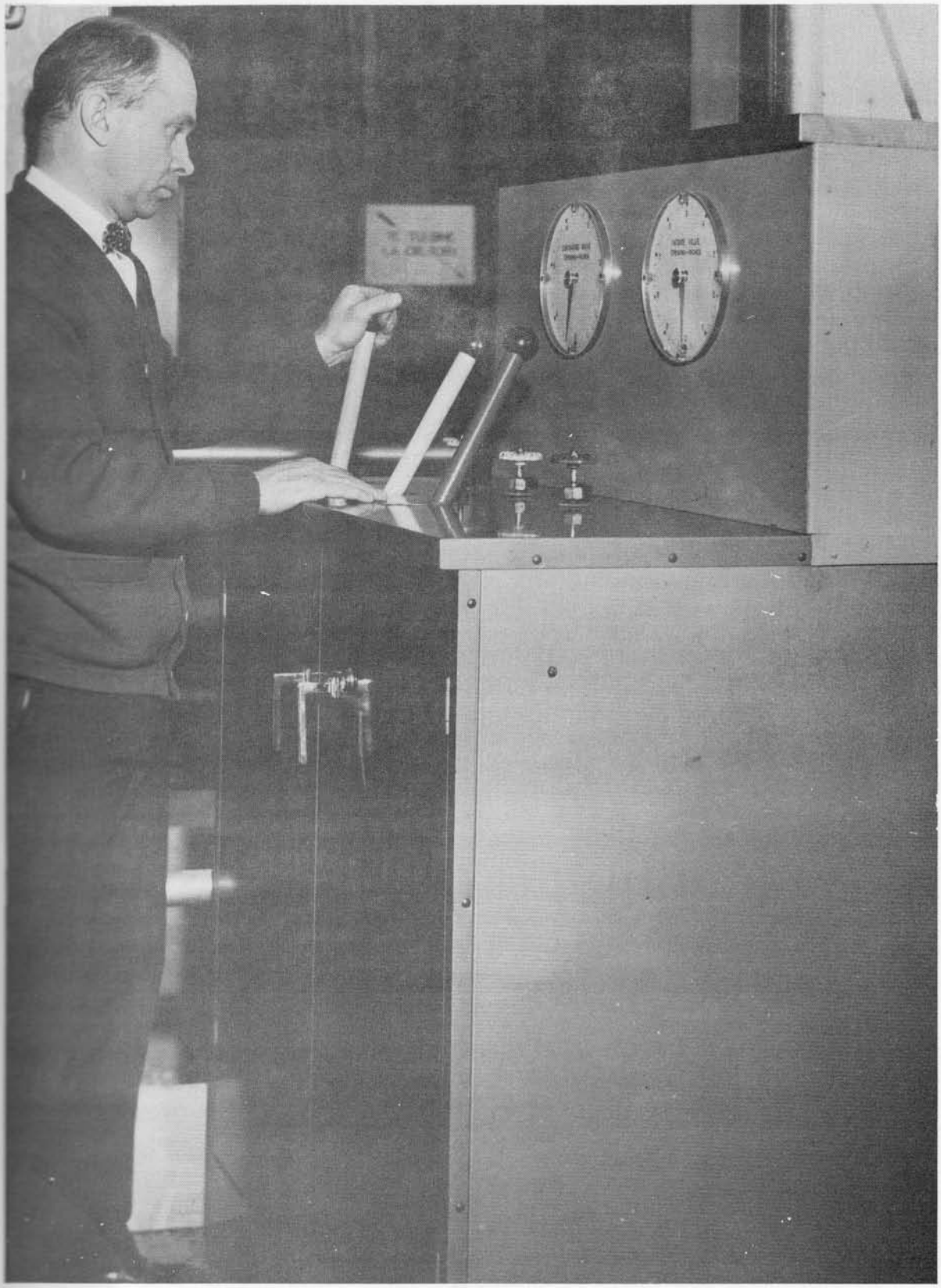

Fig. 5 – The Control Stand

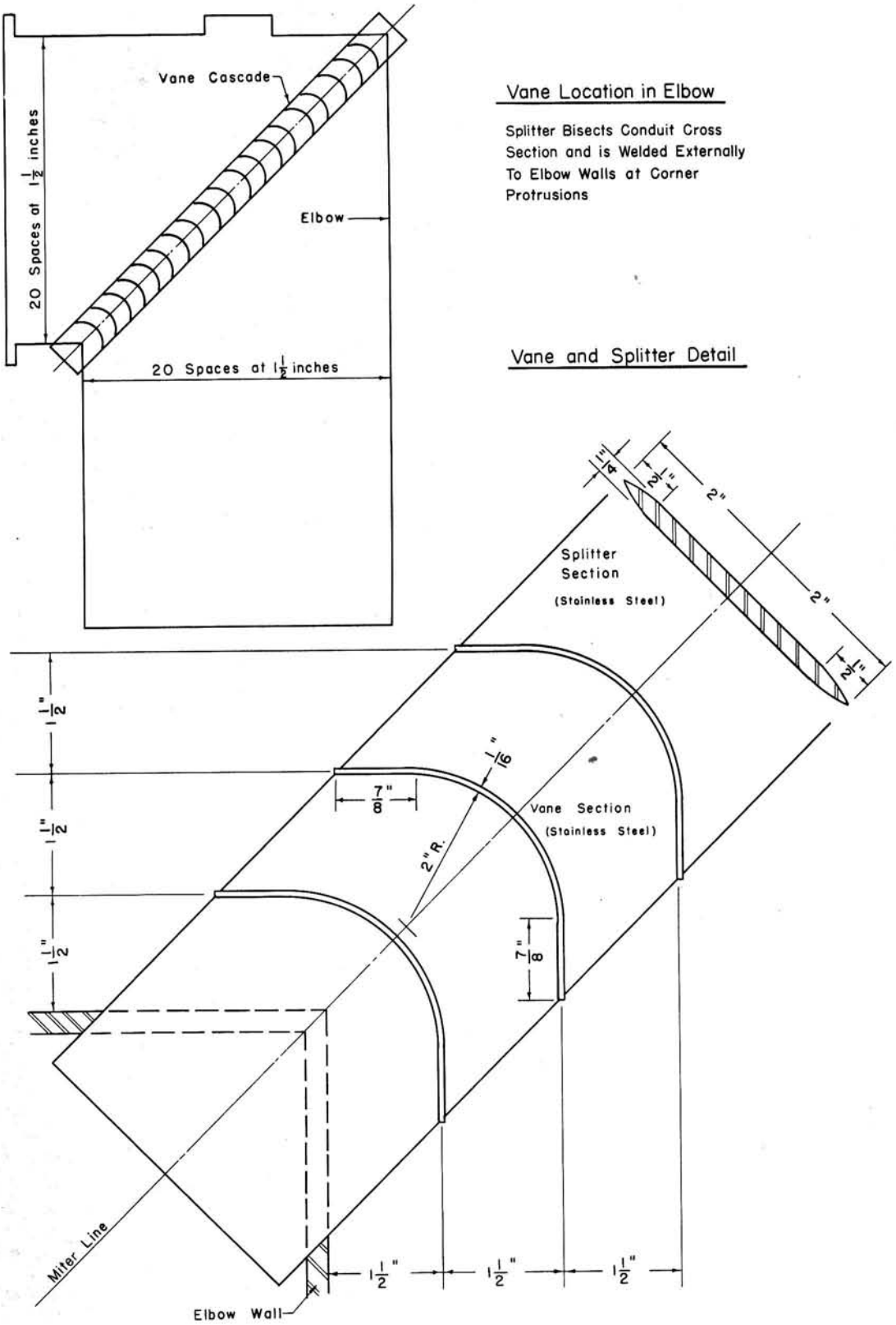

Fig. 6 - Details of Miter Elbow Guide Vanes

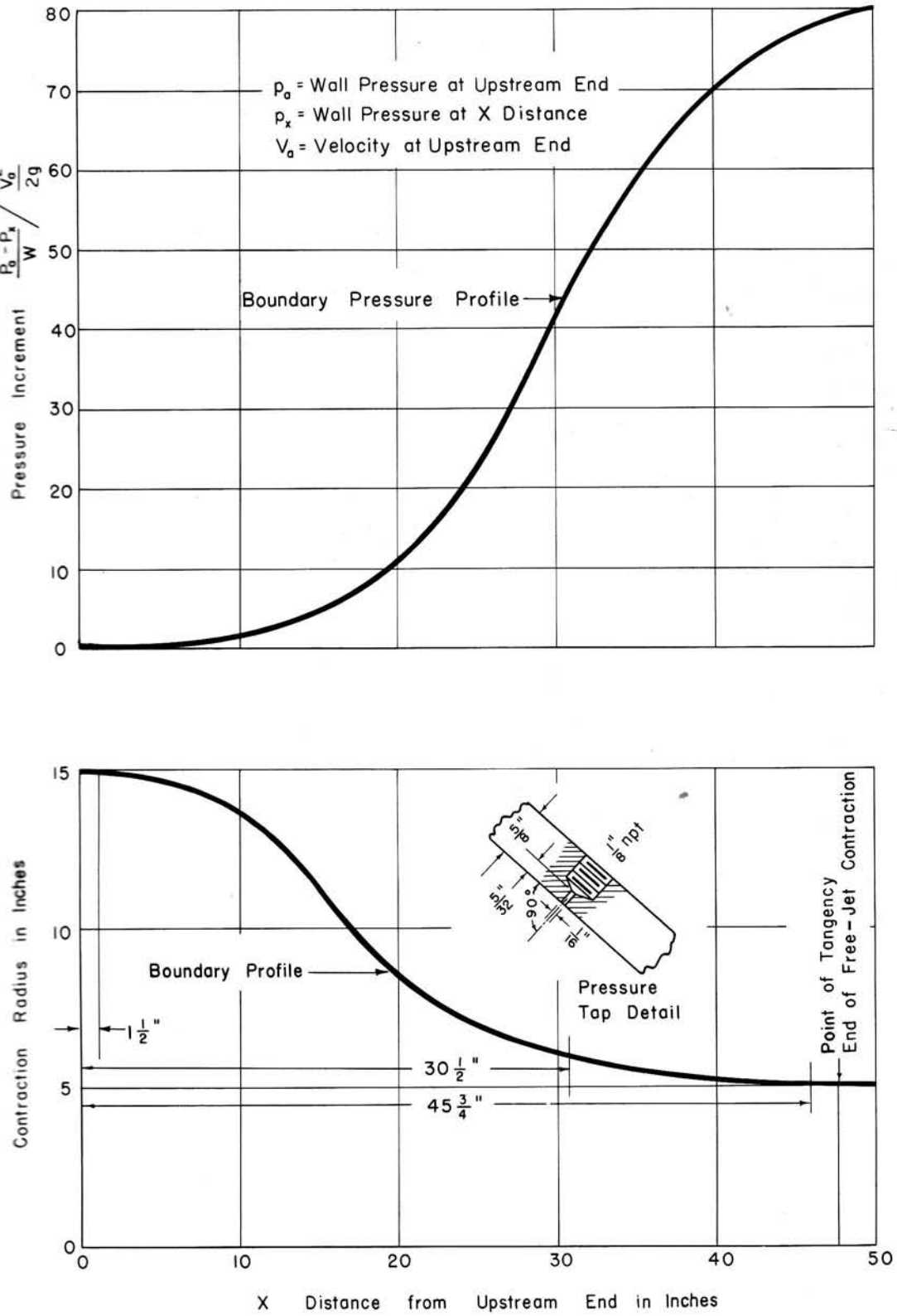

Fig. 7 – Boundary Profile and Boundary Pressure for the Axially Symmetric Nozzle

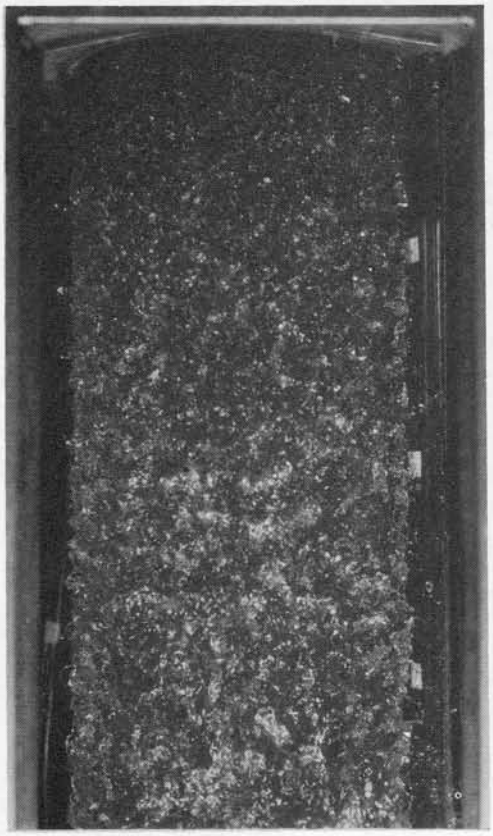

V = 26 f p s
p = Atmospheric

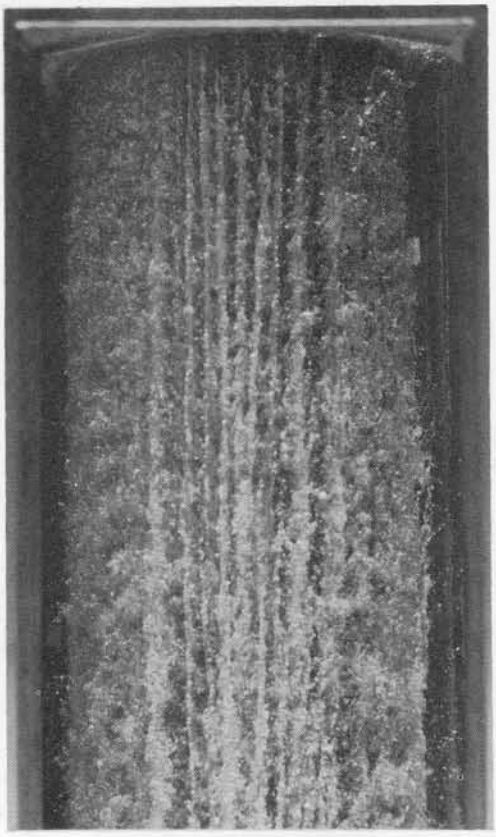

V = 48 f p s
p = Sub-Atmospheric

Fig. 8 - 10-in. Axially Symmetric Jet

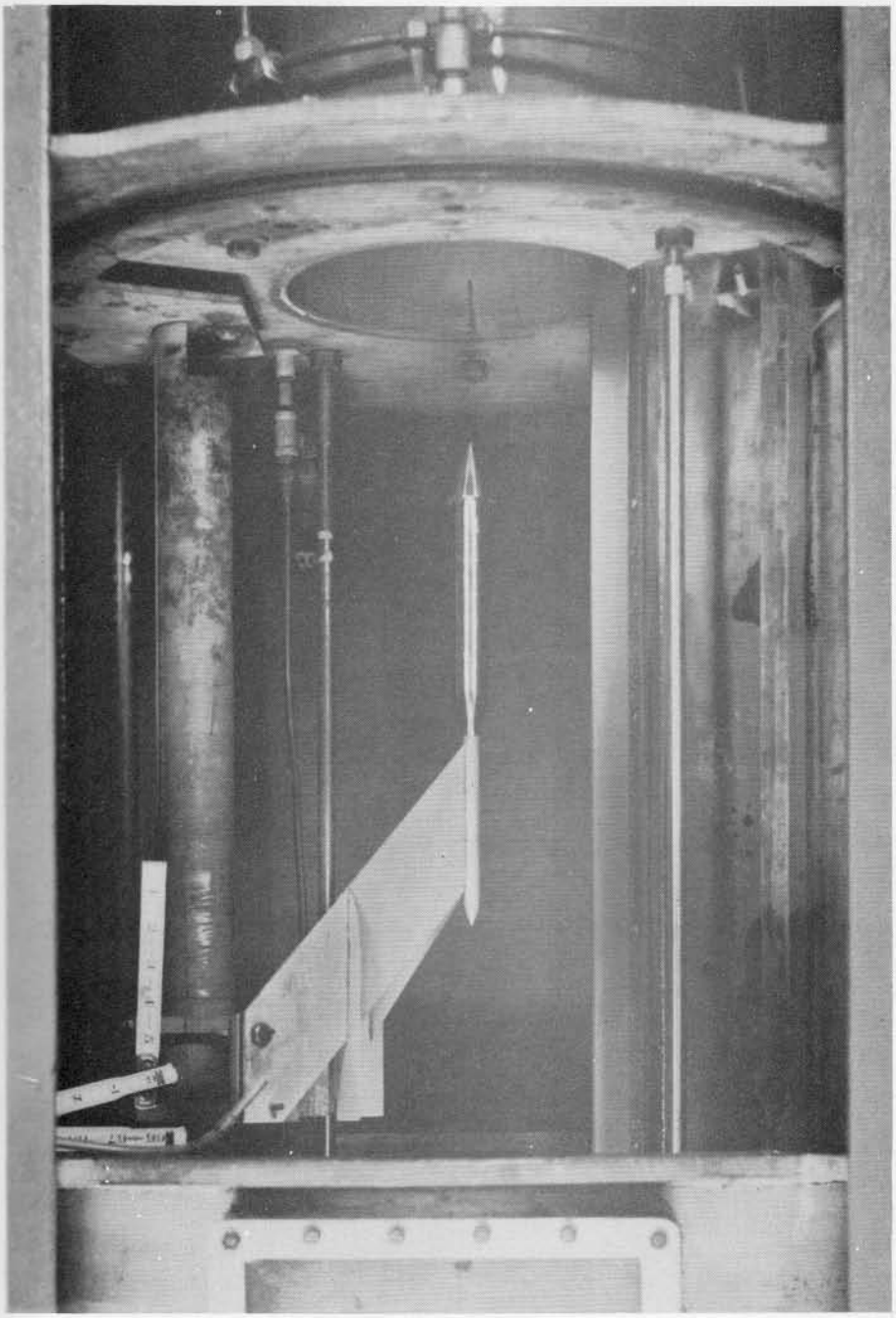

Fig. 9 - Test-Body Support System
in the Axially Symmetric Test Section

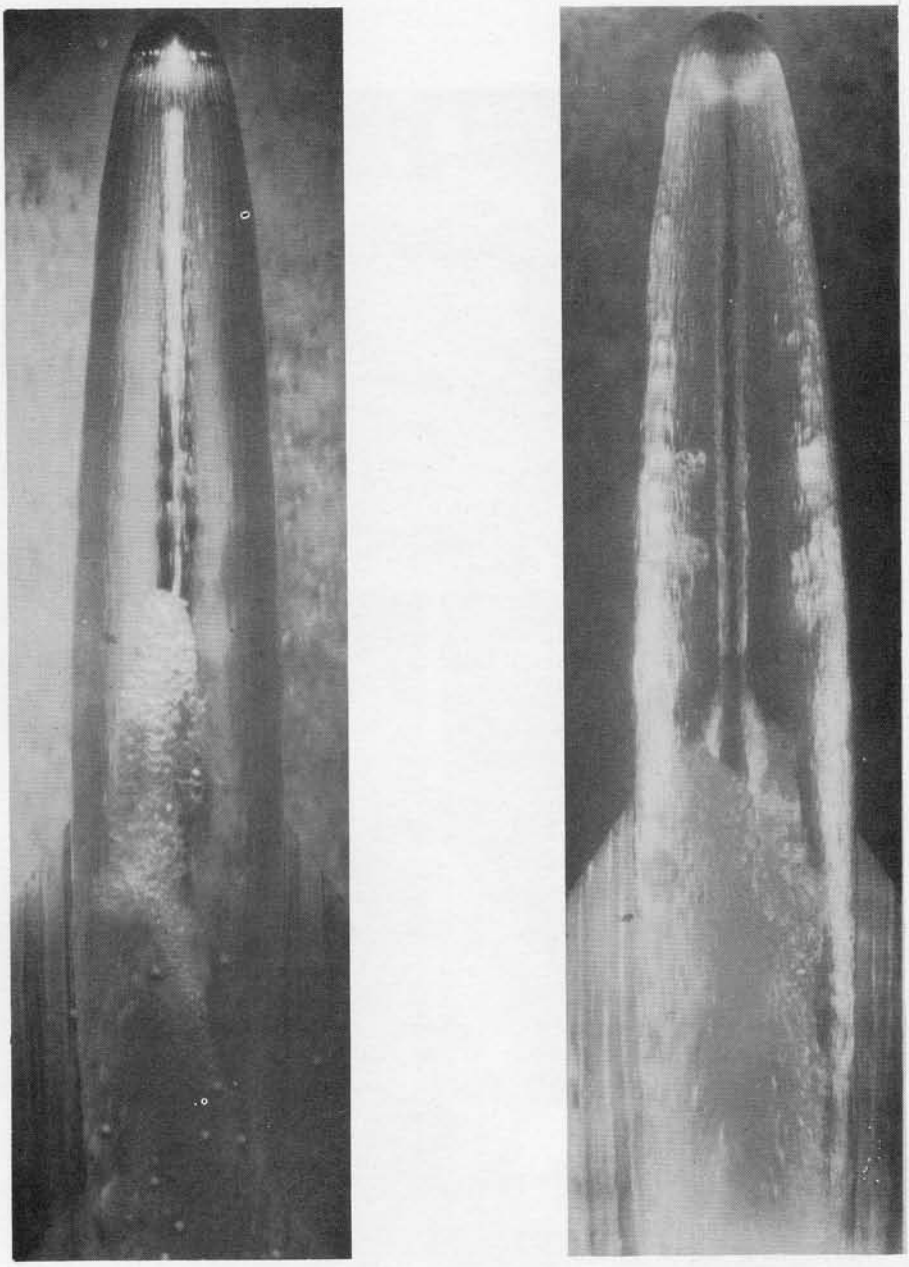

(a)
Front Lighted

(b)
Side Lighted

Exposure Time = 1/2500 sec

σ = 0.06

Fig. 10 - Vapor Cavity on a Sphere
in the Axially Symmetric Jet

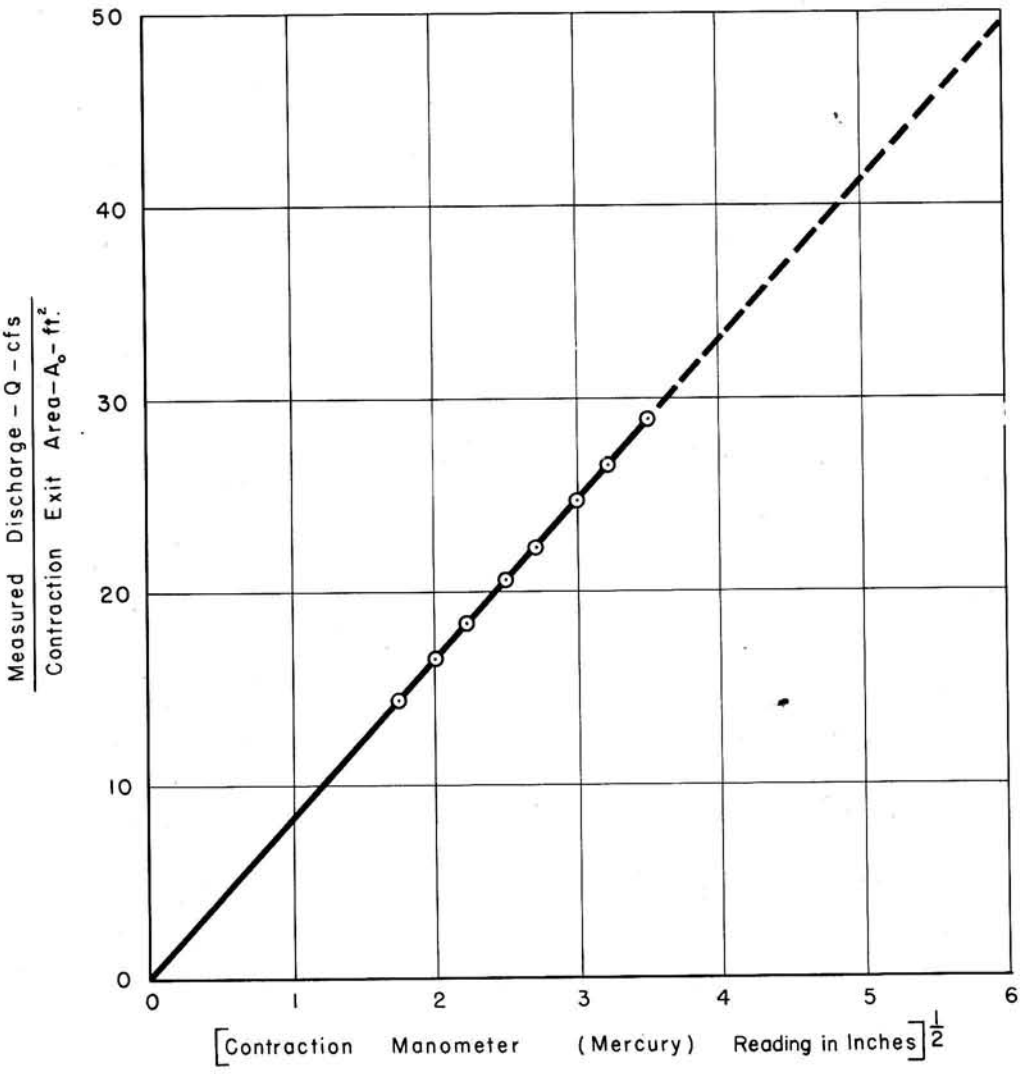

Fig. 11 – Velocity Calibration of Axially Symmetric Contraction

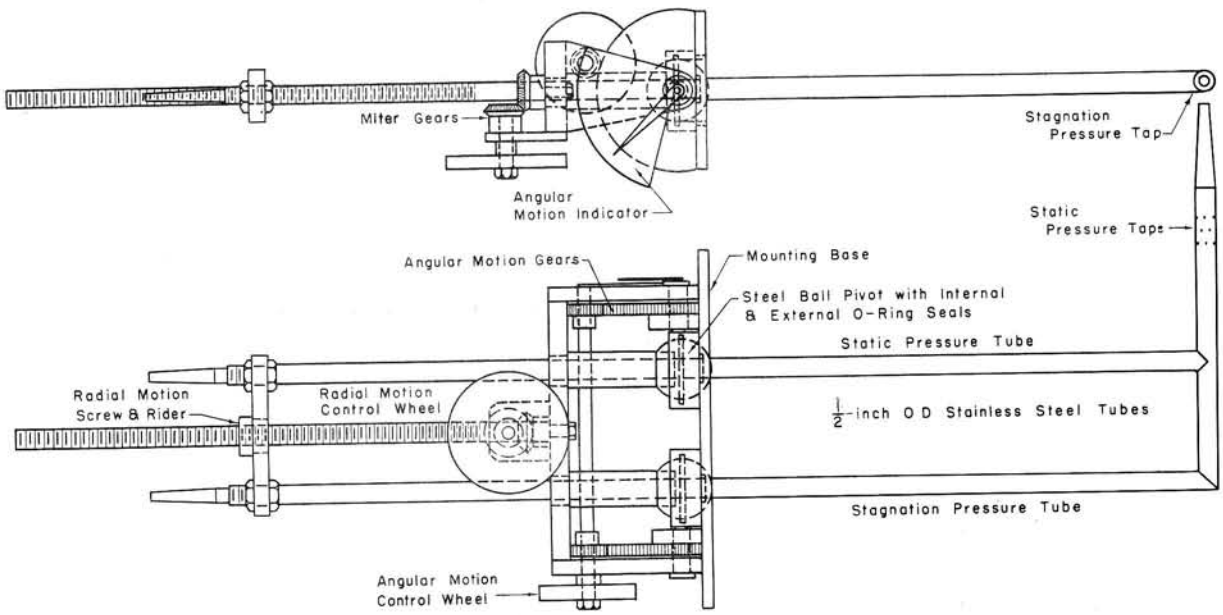

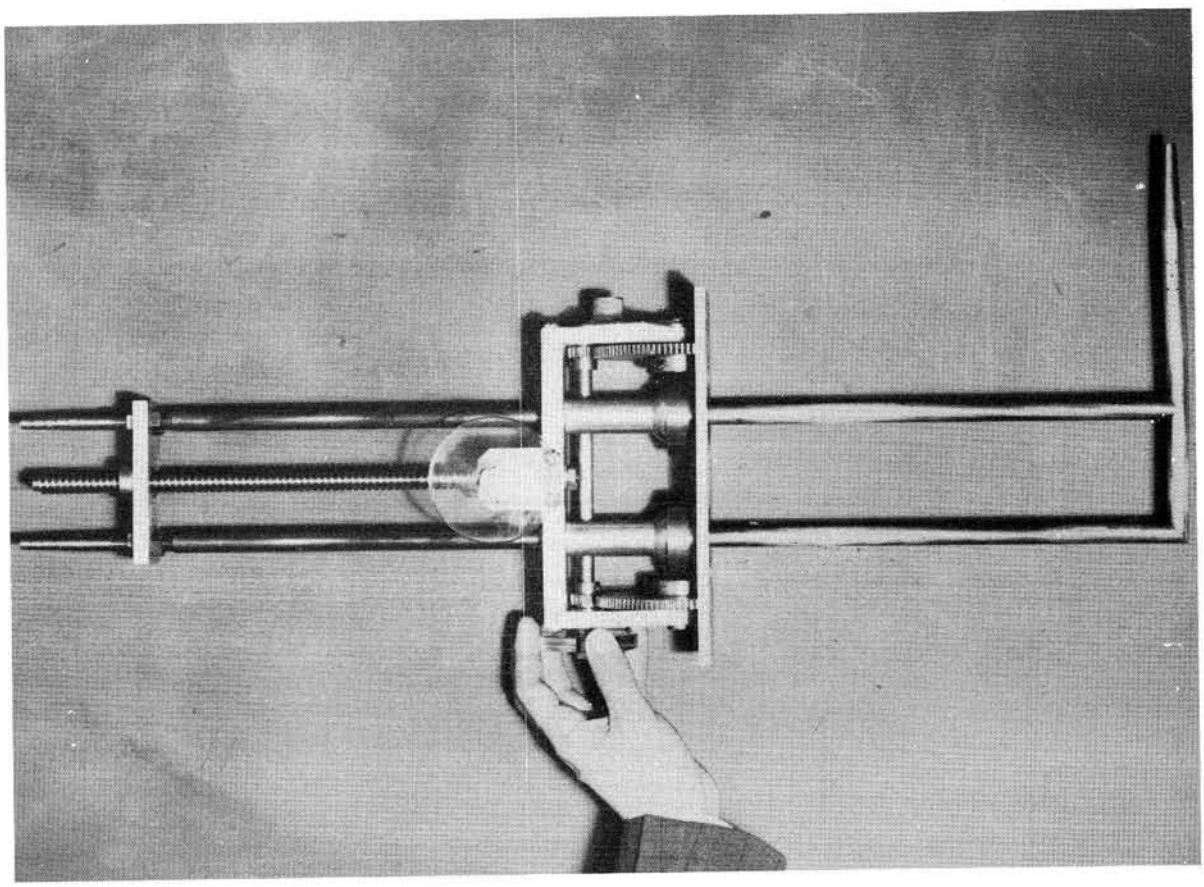

Fig. 12 - The Pitot-Static Tube

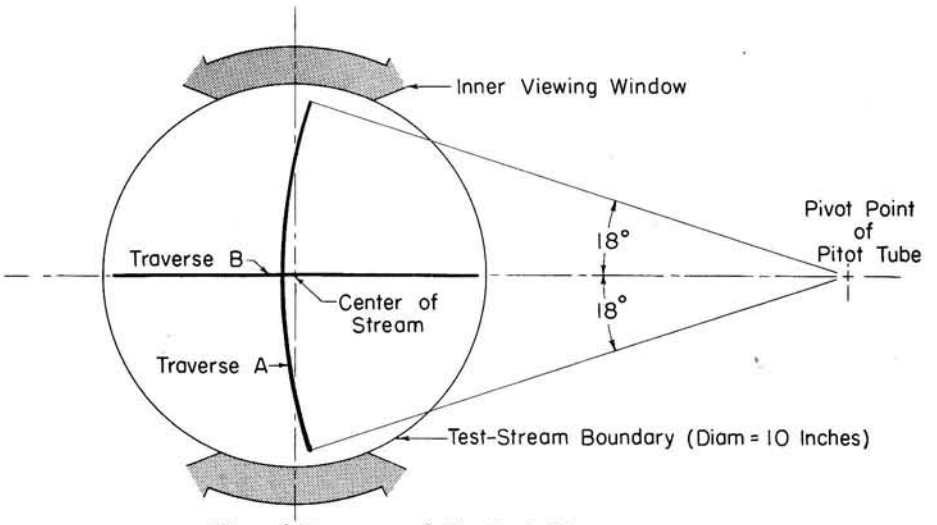

Plan of Traverses of the Test Stream
(Vertical Location – $2\frac{3}{4}$ Inches Below Contraction Exit)

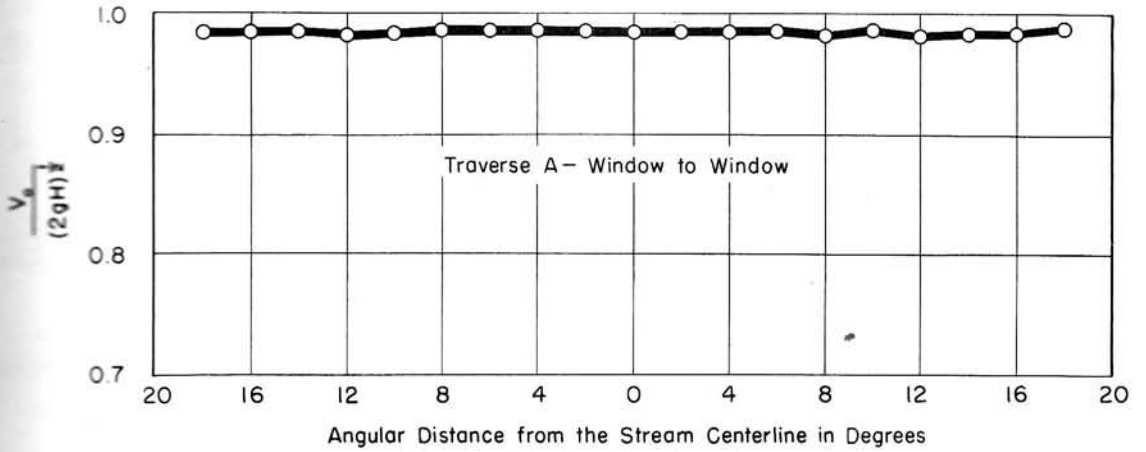

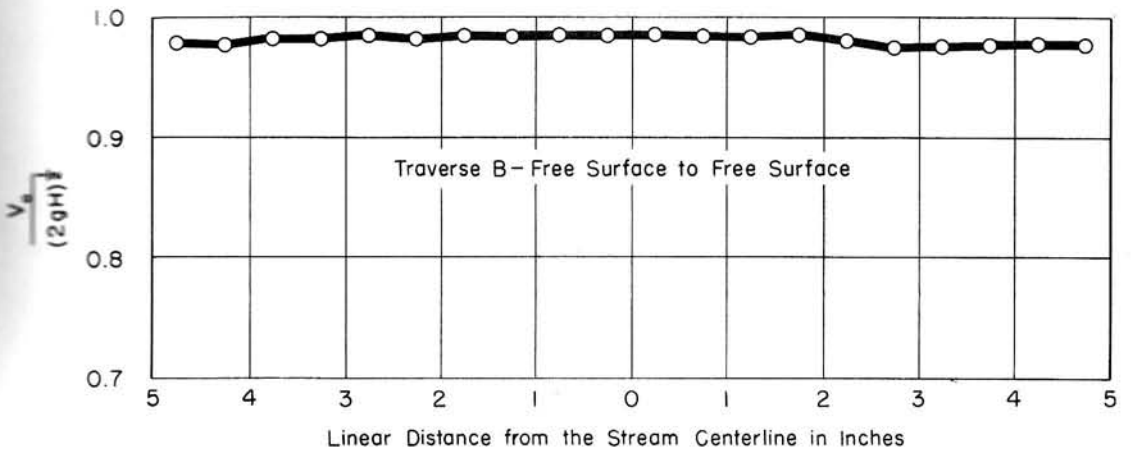

Fig. 13 – Velocity Survey in the Axially Symmetric Jet

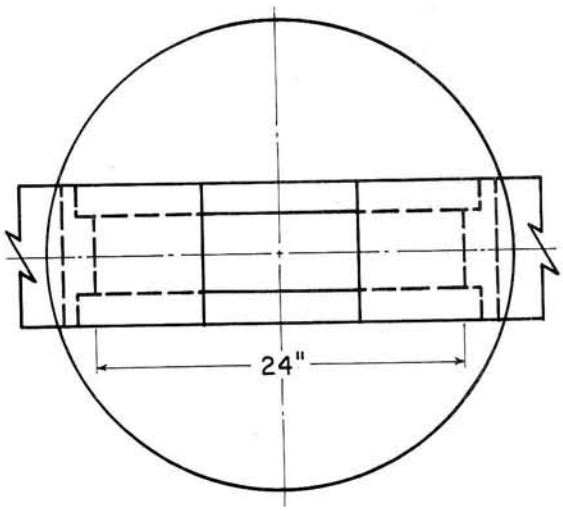

Width of Jet in Inches

B	b_∞	b
8.06	5.00	5.00
9.63	6.00	6.01
12.63	8.00	8.03
15.47	10.00	10.06
18.09	12.00	12.15
21.62	15.00	15.28
22.73	16.00	16.36

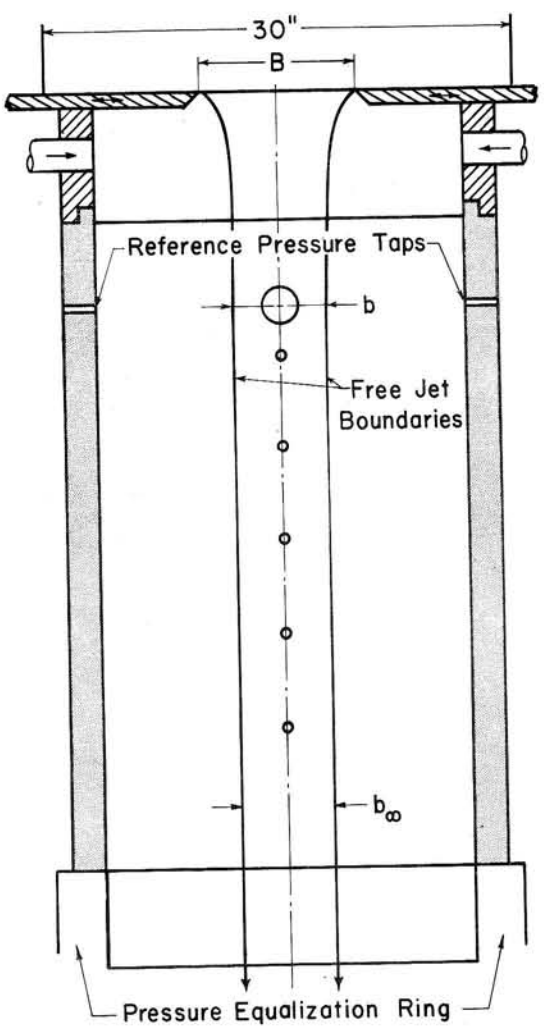

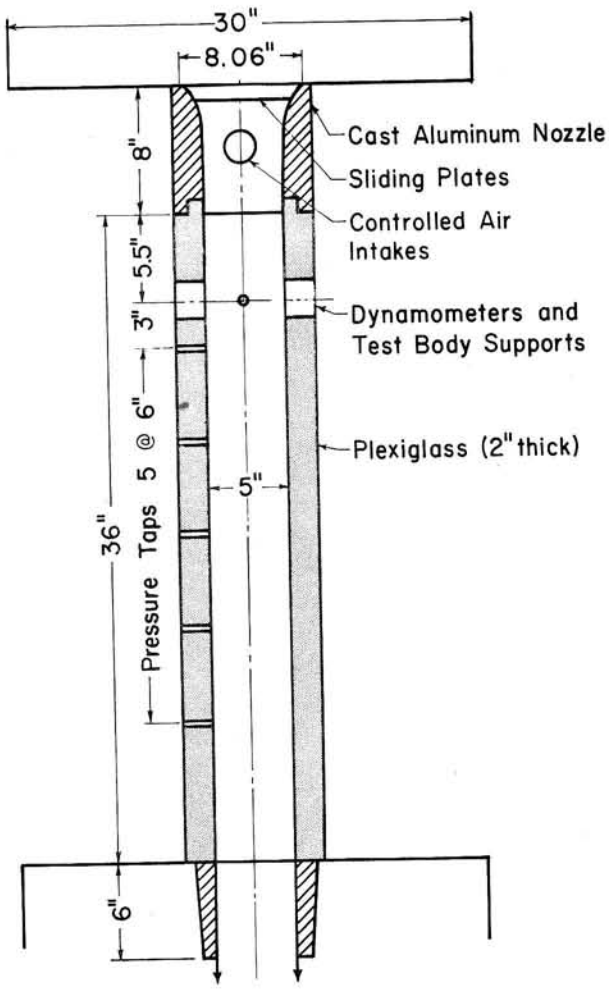

Fig. 14 - Schematic Drawing of Two-Dimensional Test Section and Appurtenances

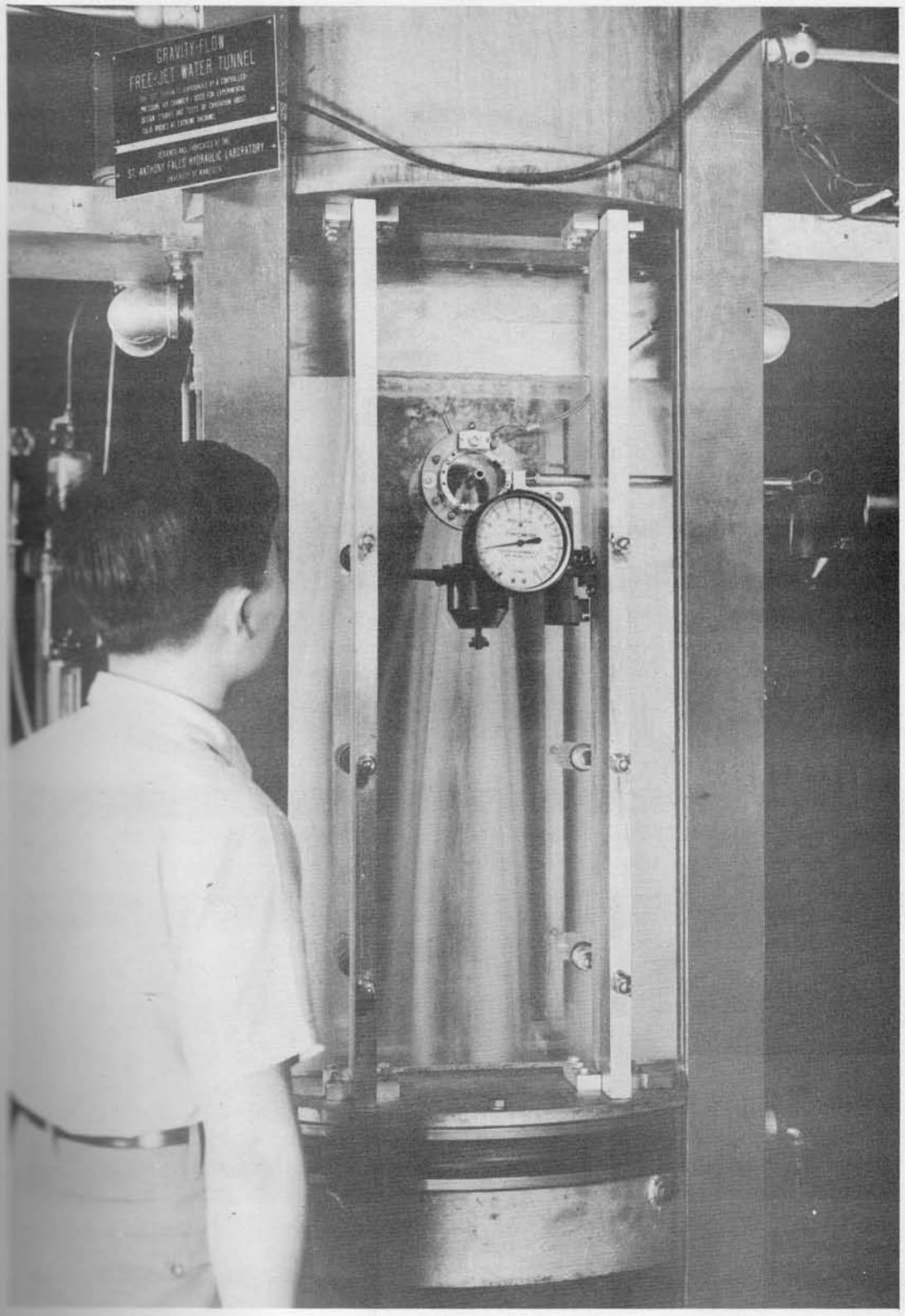

Fig. 15 - Flow in Two-Dimensional Test Section with Circular Cylinder and Dynamometer

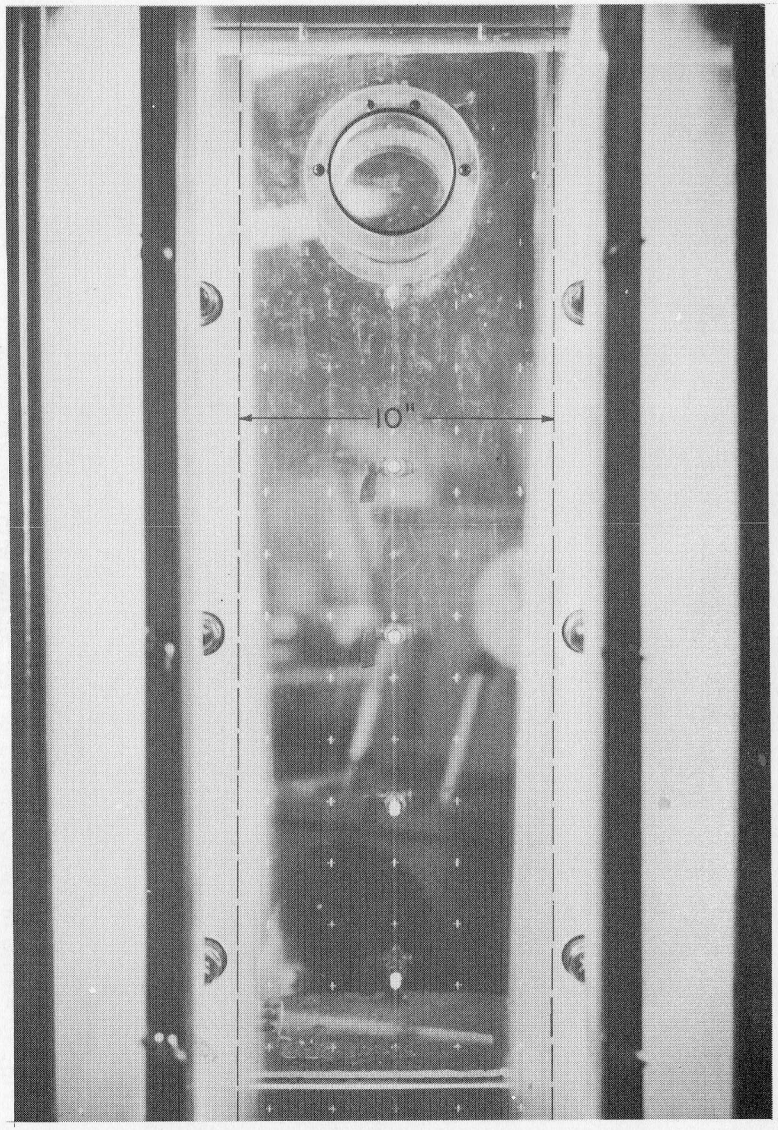

Fig. 16 – Flow in Two-Dimensional Test Section without Test Body

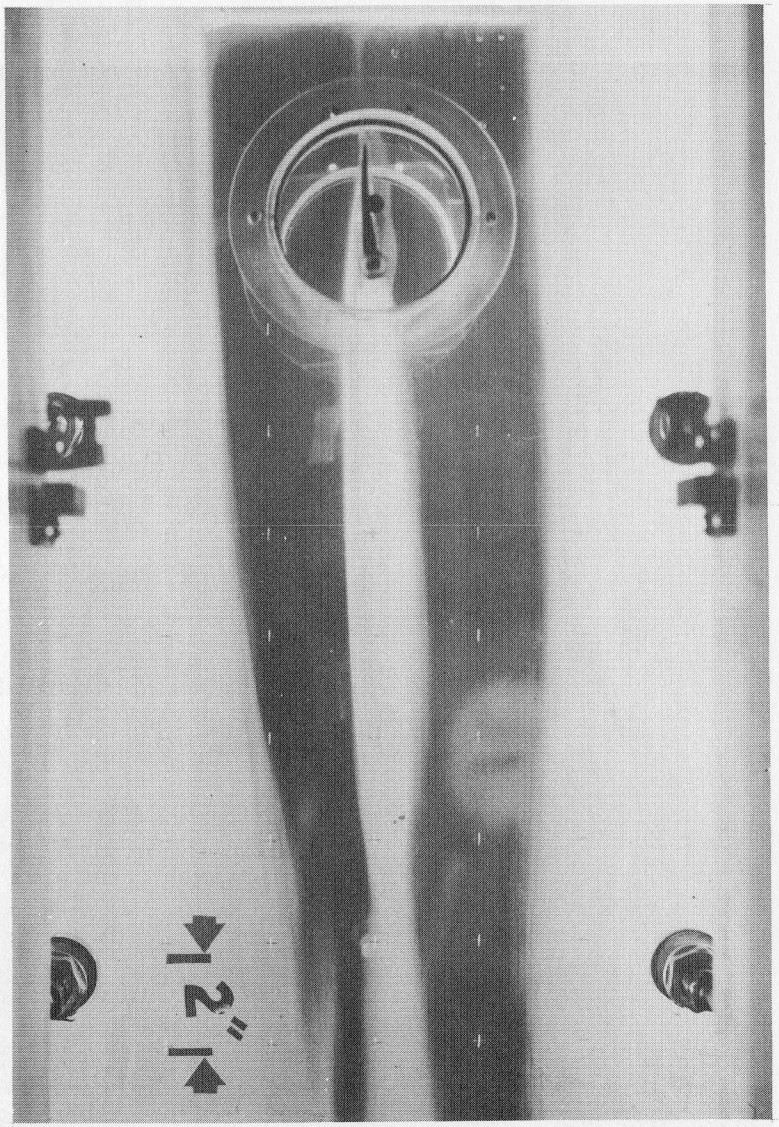

Fig. 17 – Flow in Two-Dimensional Test Section with Lifting Foil but without Dynamometer

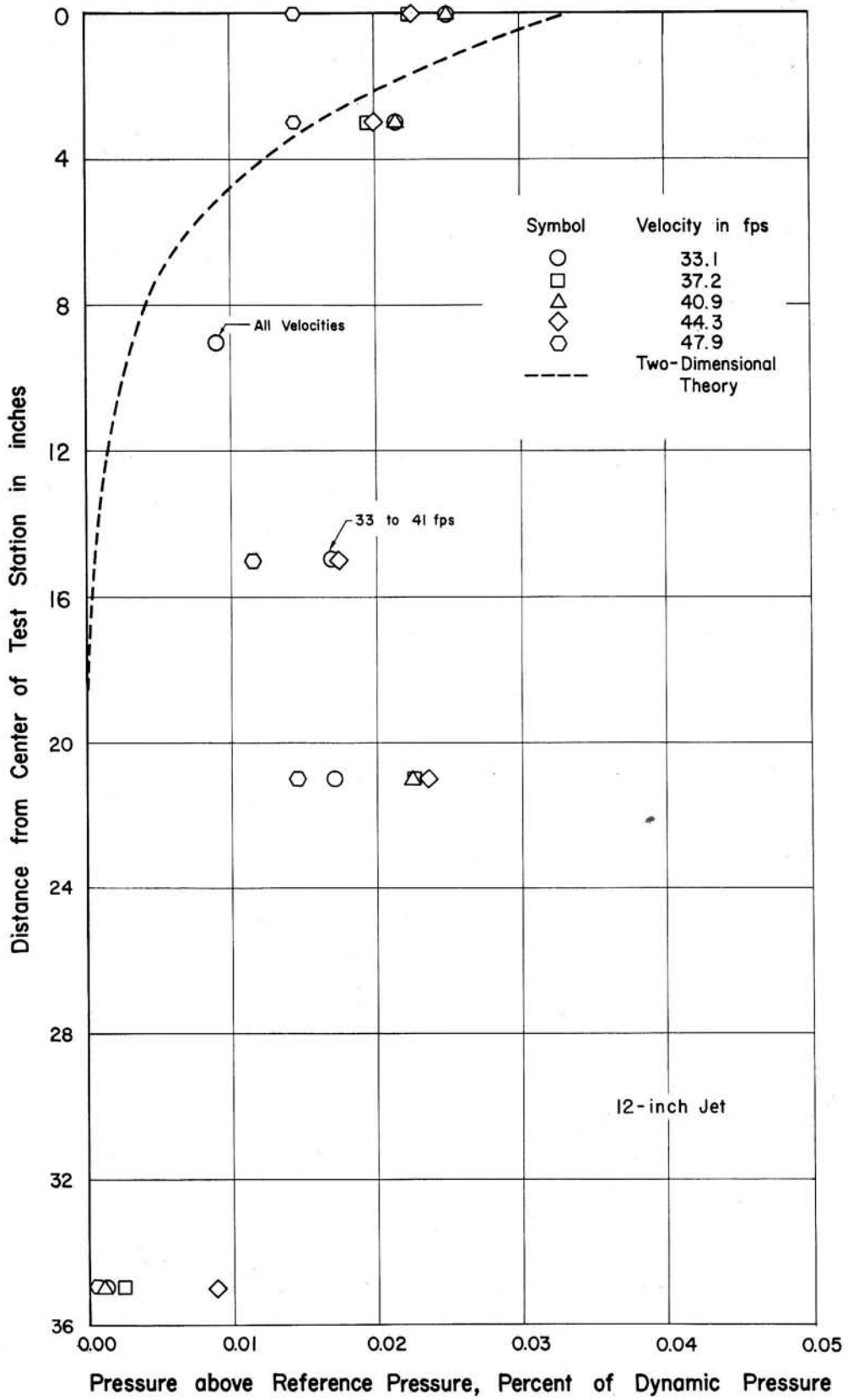

Fig. 18 - Typical Pressure Distribution in Two-Dimensional Jet without Test Body

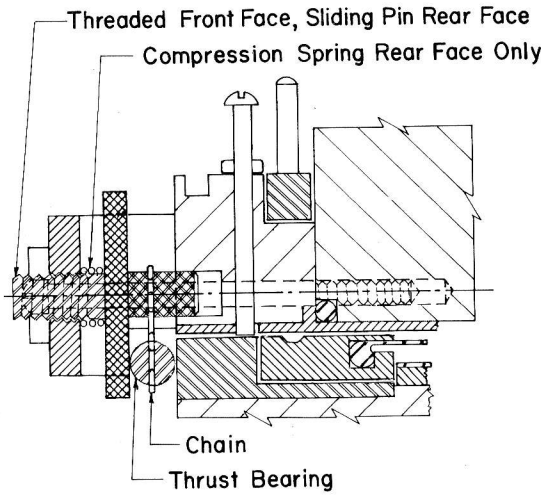

Section C-C

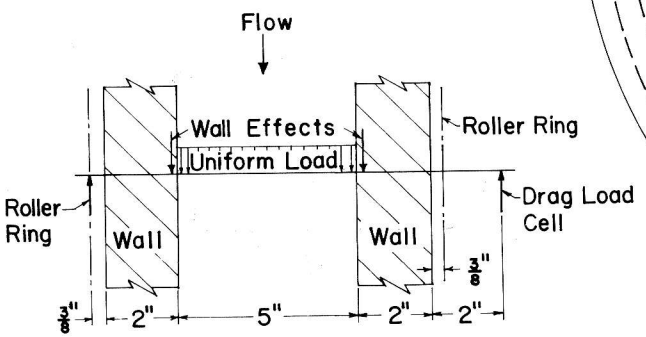

Drag Load Distribution

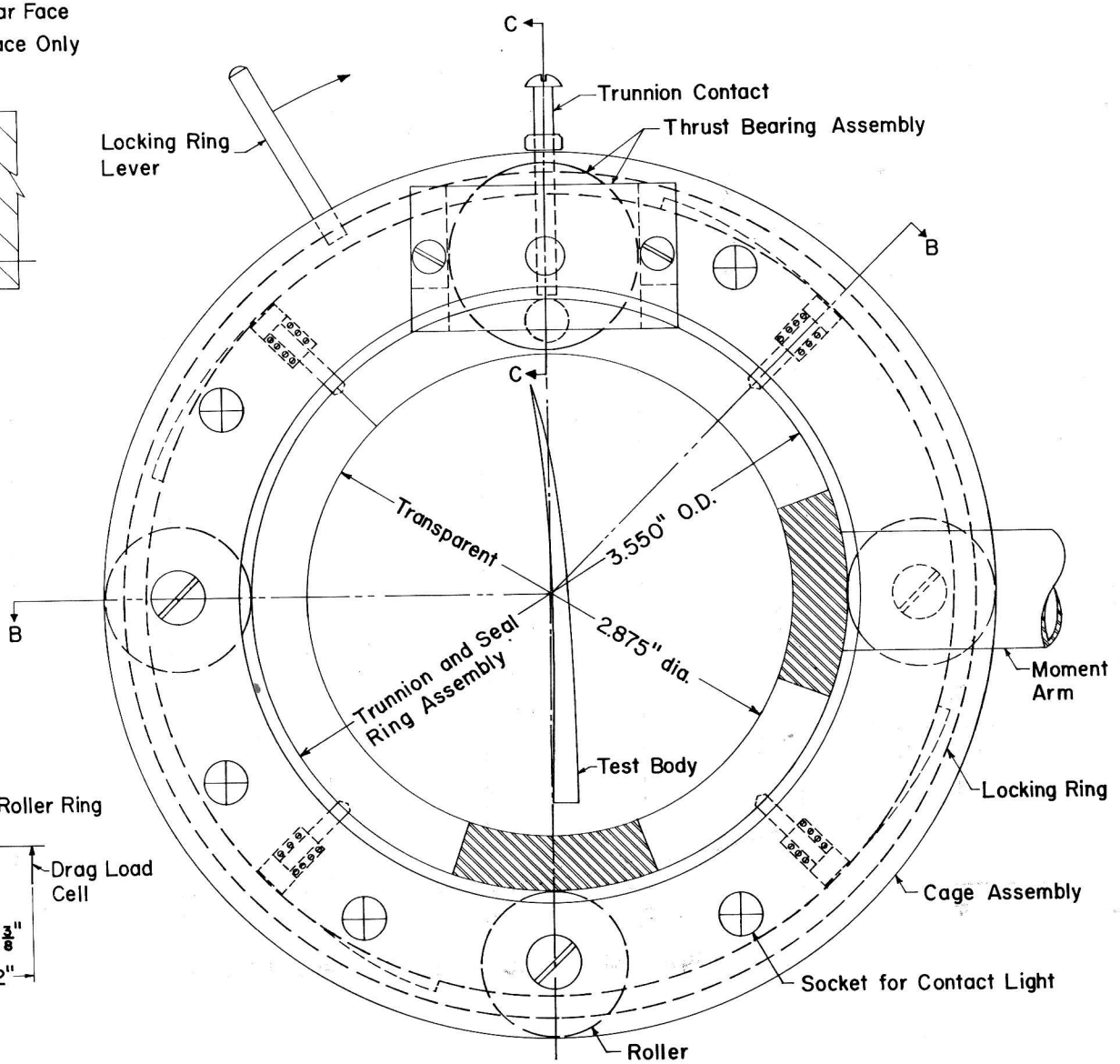

Section A-A

See Elevation View on Facing Page

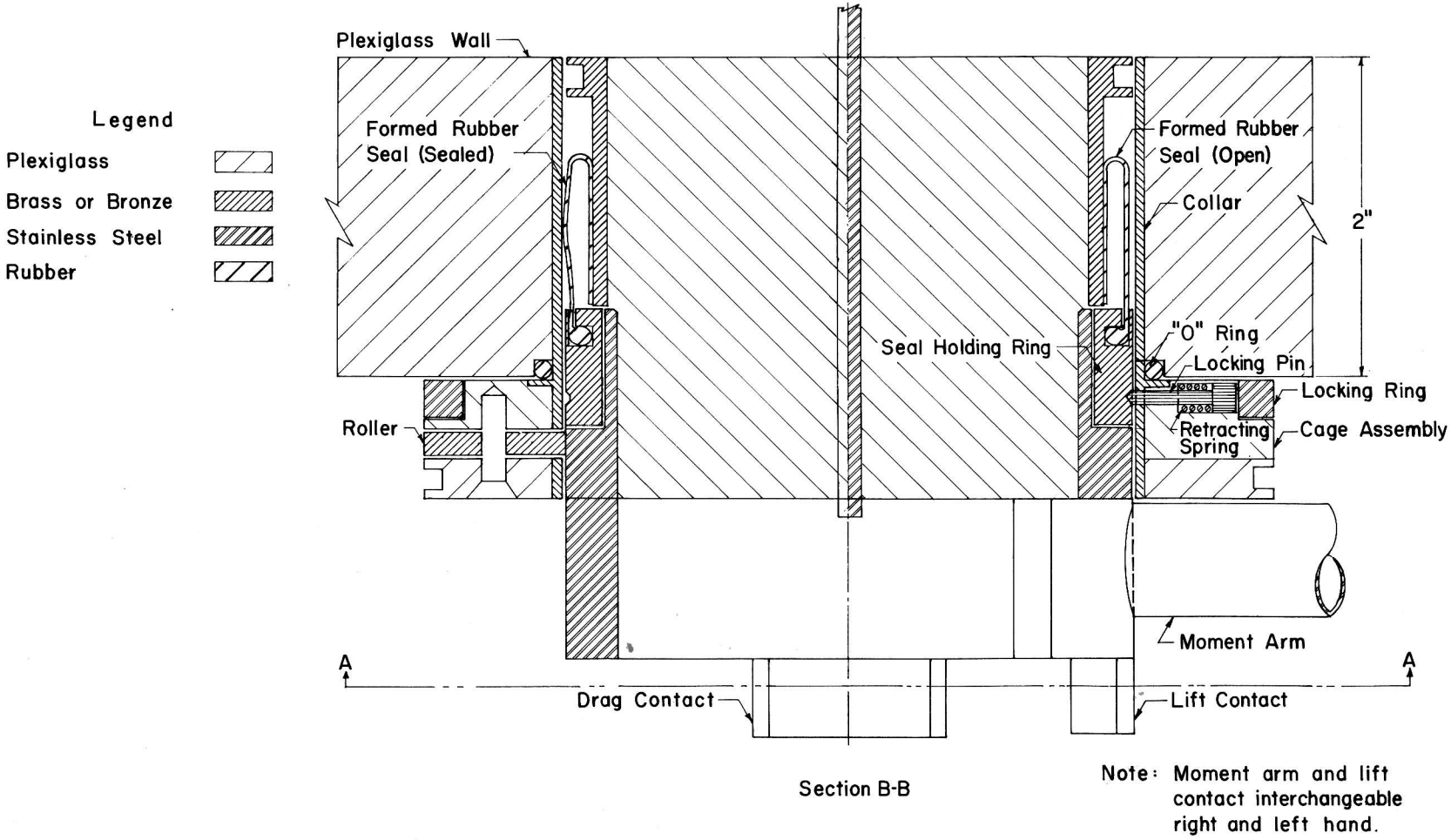

Fig. 19 - Dynamometer Arrangement

DISTRIBUTION LIST FOR TECHNICAL PAPER NO. 24-B

of the St. Anthony Falls Hydraulic Laboratory

Copies	Organization
3	Chief of Naval Research, Department of the Navy, Washington 25, D. C., Attn: 1 - Code 438 1 - Code 463 1 - Code 466
1	Commanding Officer, Office of Naval Research Branch Office, The John Crerar Library Building, 86 East Randolph Street, Chicago 1, Illinois.
1	Commanding Officer, Office of Naval Research Branch Office, 346 Broadway, New York 13, New York.
1	Commanding Officer, Office of Naval Research Branch Office, 1030 East Green Street, Pasadena 1, California.
1	Commanding Officer, Office of Naval Research Branch Office, 1000 Geary Street, San Francisco 9, California.
25	Commanding Officer, Office of Naval Research, Navy 100, Fleet Post Office, New York, New York.
6	Director, Naval Research Laboratory, Washington 25, D. C., Attn: Technical Information Office (Code 2000).
2	Chief, Bureau of Aeronautics, Department of the Navy, Washington 25, D. C., Attn: 1 - Aero and Hydro Branch (Code AD-3) 1 - Research Division (Code RS)
2	Chief, Bureau of Ordnance, Department of the Navy, Washington 25, D. C., Attn: 1 - Assistant for Aero, Hydro, and Ballistics (Code Re03) 1 - Underwater Missile Branch (Code ReU1)
5	Chief, Bureau of Ships, Department of the Navy, Washington 25, D. C., Attn: 1 - Technical Assistant to Chief of Bureau (Code 106) 1 - Research and Development Division (Code 310) 1 - Technical Library (Code 312) 1 - Preliminary Design Branch (Code 420) 1 - Propellers and Shafting (Code 554)
5	Commanding Officer and Director, David Taylor Model Basin, Washington 7, D. C., Attn: 1 - Library Branch (Code 142) 1 - Technical Director for Hydromechanics Laboratory (Code 500) 1 - Contract Research Administrator (Code 513)

Copies	Organization
	1 - Propeller Branch (Code 526) 1 - Fluid Dynamics Branch (Code 591)
1	Commander, U. S. Naval Ordnance Test Station, China Lake, California, Attn: Library Division (Code 753).
1	Officer-in-Charge, Pasadena Annex, U. S. Naval Ordnance Test Station, 3202 E. Foothill Boulevard, Pasadena, California, Attn: Library Section (Code P80962).
1	Commanding Officer and Director, U. S. Naval Engineering Experiment Station, Annapolis, Maryland.
1	Commander, Naval Proving Ground, Dahlgren, Virginia, Attn: Technical Library Division (AAL).
1	Commander, U. S. Naval Ordnance Laboratory, White Oak, Maryland, Attn: Library Division (Desk HL).
1	Commanding Officer, U. S. Naval Underwater Ordnance Station, Newport, Rhode Island, Attn: Research Division.
1	Mr. C. R. Dennison, Coordinator of Research, Maritime Administration, 441 G Street, N. W., Washington 25, D. C.
3	National Bureau of Standards, Washington 25, D. C., Attn: 1 - Fluid Mechanics Section 1 - Dr. G. B. Schubauer 1 - Dr. G. H. Keulegan
1	National Academy of Sciences, National Research Council, 2101 Constitution Avenue, N. W., Washington, D. C.
1	Superintendent, U. S. Naval Academy, Annapolis, Maryland, Attn: Librarian.
1	Superintendent, U. S. Naval Postgraduate School, Monterey, California, Attn: Librarian.
1	Superintendent, U. S. Merchant Marine Academy, Kings Point, Long Island, New York, Attn: Captain L. S. McCready, Head, Department of Engineering.
1	Air Force Office of Scientific Research, Mechanics Division, Washington 25, D. C.
1	Commanding Officer, Office of Ordnance Research, Box CM, Duke Station, Durham, North Carolina.
5	Director of Research, National Aeronautics and Space Agency, 1512 H Street, N. W., Washington 25, D. C.

Copies	Organization
1	Mr. J. B. Parkinson, Langley Aeronautical Laboratory, National Aeronautics and Space Administration, Langley Field, Virginia.
1	Director, Engineering Sciences Division, National Science Foundation, 1520 H Street, N. W., Washington, D. C.
5	Document Service Center, Armed Services Technical Information Agency, Arlington Hall Station, Arlington 12, Virginia.
1	Office of Technical Services, Department of Commerce, Washington 25, D. C.
4	California Institute of Technology, Pasadena 4, California. Attn: 1 - Professor C. B. Millikan 1 - Professor T. Y. Wu 1 - Professor A. Acosta 1 - Hydro Lab
3	University of California, Berkeley 4, California, Attn: 1 - Department of Engineering 1 - Professor H. A. Schade 1 - Professor J. V. Wehausen
1	Director, Scripps Institution of Oceanography, University of California, La Jolla, California.
1	Director, Woods Hole Oceanographic Institute, Woods Hole, Massachusetts.
1	Professor M. Albertson, Department of Civil Engineering, Colorado State University, Fort Collins, Colorado.
2	Iowa Institute of Hydraulic Research, State University of Iowa, Iowa City, Iowa, Attn: 1 - Professor H. Rouse, Director 1 - Professor L. Landweber
2	Harvard University, Cambridge 38, Massachusetts, Attn: 1 - Professor G. Birkhoff (Department of Mathematics) 1 - Professor G. F. Carrier (Division of Engineering and Applied Physics)
2	Massachusetts Institute of Technology, Cambridge 39, Massachusetts, Attn: 1 - Professor L. Troost (Department of N.A. and M.E.) 1 - Professor A. T. Ippen (Hydro Labratory)
3	University of Michigan, Ann Arbor, Michigan, Attn: 1 - Professor R. B. Couch (Department of N.A. and M.E.) 1 - Professor C.-S. Yih (Department of Engineering Mechanics) 1 - Professor V. Streeter (Department of Civil Engineering)

Copies	Organization
1	Director, St. Anthony Falls Hydraulic Laboratory, University of Minnesota, Minneapolis 14, Minnesota.
1	Director, Alden Hydraulic Laboratory, Worcester Polytechnic Institute, Worcester, Massachusetts.
1	Director, Ordnance Research Laboratory, Pennsylvania State University, University Park, Pennsylvania.
1	Director, Institute of Mathematical Sciences, New York University, 25 Waverly Place, New York 3, New York.
1	Professor J. J. Foody, Engineering Department, New York State University Maritime College, Fort Schulyer, New York.
1	Technical Library, Webb Institute of Naval Architecture, Crescent Beach Road, Glen Cove, Long Island, New York.
1	Professor W. R. Sears, Graduate School of Aeronautical Engineering, Cornell University, Ithaca, New York.
1	Professor S. Corrsin, Chairman, Mechanical Engineering Department, The Johns Hopkins University, Baltimore 18, Maryland.
1	Society of Naval Architects and Marine Engineers, 74 Trinity Place, New York 6, New York.
1	Engineering Societies Library, 29 West 39th Street, New York 18, New York.
3	Stevens Institute of Technology, Experimental Towing Tank, 711 Hudson Street, Hoboken, New Jersey. Attn: 1 - Technical Director 1 - Dr. P. Kaplan 1 - Mr. D. Savitsky
1	Dr. J. Kotik, Technical Research Group, 17 Union Square West, New York 3, New York.
1	Director, Institute for Fluid Mechanics and Applied Mathematics, University of Maryland, College Park, Maryland.
1	Division of Applied Mathematics, Brown University, Providence 12, Rhode Island.
1	Hydrodynamics Laboratory, National Research Council, Ottawa, Canada.
1	Professor L. M. Milne-Thomson, Mathematical Research Center, 1118 W. Johnson Center, Madison 6, Wisconsin.
1	Dr. J. M. Robertson, Department of Theoretical and Applied Mechanics, College of Engineering, University of Illinois, Urbana, Illinois.

Copies	Organization
2	Stanford University, Stanford, California, Attn: 1 - Professor J. K. Vennard (Civil Engineering Department) 1 - Applied Mathematics and Statistics Laboratory
1	Professor J. B. Herbich, Civil Engineering Department, Lehigh University, Bethelehem, Pennsylvania.
1	Dean J. S. McNown, Department of Applied Mechanics, University of Kansas, Lawrence, Kansas.
1	Professor A. G. Strandhagen, Department of Engineering Mechanics, University of Notre Dame, Notre Dame, Indiana.
2	Polytechnic Institute of Brooklyn, Department of Aeronautical Engineering and Applied Mechanics, 333 Jay Street, Brooklyn 1, New York, Attn: 1 - Professor A. Ferri 1 - Professor H. Reissner
1	Professor H. Cohen, Department of Mathematics, Rensselaer Polytechnic Institute, Troy, New York.
1	Professor D. Gilbarg, Applied Mathematics and Statistics Laboratory, Stanford University, Stanford, California.
1	Mr. Leo Geyer, Chief of Preliminary Design, Grumman Aircraft Engineering Corporation, Bethpage, Long Island, New York.
1	Mr. W. P. Carl, Jr., Dynamic Developments, Inc., Babylon, Long Island, New York.
1	EDO Corporation, College Point, Long Island, New York.
1	Mr. H. E. Brooke, Hydrodynamics Laboratory, Convair, San Diego 12, California.
1	Miami Shipbuilding Corporation, 615 S. W. Second Avenue, Miami 36, Florida.
1	Baker Manufacturing Company, Evansville, Wisconsin.
1	Gibbs and Cox, Inc., 21 West Street, New York 16, New York.
1	Dr. H. Reichardt, Max-Planck-Institut fuer Stroemungsforschung, Goettingem, Boettingerstrasse 6/8, West Germany.
1	Director of Research, National Aeronautics and Space Administration, Lewis Research Center, 21000 Brookpark Road, Cleveland 35, Ohio.
1	Hydronautics, Inc., 200 Monroe Street, Rockville, Maryland, Attn: Mr. Phillip Eisenberg, Mr. M. P. Tulin.
1	Commanding Officer and Director, U. S. Naval Civil Engineering Laboratory, Port Hueneme, California, Attn: Code L54.